Fizyka rozbłysków słonecznych

- wykład nr XIV

Krzysztof Radziszewski

Instytut Astronomiczny, Uniwersytet Wrocławski

Magnetohyrodynamika

pętli koronalnych

c.d.

Magnetostatyka w pionowej rurze magnetycznej

Przyjmując oznaczenia jak na rysunku możemy zapisać, że całkowite ciśnienie wewnątrz rury jest równoważne ciśnieniu termicznemu na zewnątrz rury:

$$p_E = p_0 + \frac{\vec{B}_0^2}{8\pi}$$

Podstawiając:

$$p_0 = 2n_0 k_B T_0 \qquad \text{oraz} \qquad p_E = 2n_E k_B T_E$$

a także zakładając taką samą gęstość wewnątrz i na zewnątrz: $n = n_0 = n_E$, otrzymujemy zależność wiążącą siłę pola magnetycznego (B_0) i różnicę temperatur ($T_E - T_0$):

$$B_0^2 = 16\pi n k_B (T_E - T_0)$$

Magnetostatyka w pionowej rurze magnetycznej

W koronie, gdzie gęstość (*n*) spada poniżej 10^9 cm^{-3}, to samo pole magnetyczne nie może być równoważone przez obserwowaną różnicę temperatur, co ma duże znaczenie w „rozbieganiu się" pola magnetycznego wychodzącego z chromosfery do korony. Tak więc korona jest „całkowicie" wypełniona strukturami magnetycznymi.

W koronie *β* plazmowa jest znacznie mniejsza od 1, zatem przy „rządzącym" ciśnieniu magnetycznym możemy zapisać horyzontalną równowagę ciśnienia wyrażoną za pomocą parametrów *β:*

$$\frac{\vec{B}_0}{\vec{B}_E} = \left(\frac{1+\beta_E}{1+\beta_0} \right)^{\frac{1}{2}}$$

Magnetostatyka w pionowej rurze magnetycznej

$$\frac{\vec{B}_0}{\vec{B}_E} = \left(\frac{1+\beta_E}{1+\beta_0} \right)^{\frac{1}{2}}$$

W przypadku warunków koronowych (β_E << 1, β_0 << 1) różnica między polem magnetycznym wewnątrz rury (B_0) i na zewnątrz (B_E) jest zawsze mała.

Np: dla typowej plazmy koronalnej (B_E = 100 G, n_e = 10^9 cm^{-3}, T_e = 10^6 K parametr β-plazmowa jest równy β_e = 0,00035.

Przy zmianie gęstości w pętli koronalnej o dwa rzędy wielkości (n_0 = 10^{11} cm^{-3}), parametr β-plzmowa wynosi β_0 = 0,035 (wymaga to zmniejszenia wewnętrznego pola magnetycznego jedynie o B_0/B_E = 0,983 aby zrównoważyć ciśnienie termiczne.

Taki efekt zmiany pola (o 2%, przy zachowanym polu w przekroju pętli) może być spowodowany rozszerzeniem pętli o około 1% (tak małe rozszerzenia pętli nie są obecnie mierzalne obserwacyjnie).

Niestabilności MHD w pętlach koronalnych

Table 6.1: Overview of HD and MHD instabilities in coronal loops.

Instability	Unstable condition
1) Interchange or Pressure-Driven Instabilities:	
1.1. Rayleigh–Taylor instability:	
1.1.1 Hydrodynamic:	$\mathbf{g} \cdot \nabla n_0 < 0$
1.1.2 Hydromagnetic (Kruskal–Schwarzschild):	$\mathbf{k} \cdot \mathbf{B} = 0$
1.1.3 Hydromagnetic (Parker instability):	$\mathbf{k} \cdot \mathbf{B} \neq 0$
1.2) Kelvin–Helmholtz instability:	
1.2.1 Hydromagnetic:	$\mathbf{v}_1 > \mathbf{v}_{A,2}$
1.3) Ballooning instability:	$\mathbf{j} \times \mathbf{B} > \rho \mathbf{g}$
2) Thermal Instabilities:	
2.1) Convective instabilities:	$(dT/dz)_{crit}$
2.2) Radiatively-driven thermal instabilities:	$\tau_{cond} > \tau_{rad}$
2.3) Heating-driven thermal instabilities:	$s_H/L < 1/3$
3) Resistive Instabilities:	
3.1. Gravitational mode:	$F_{grav} > (\mathbf{j} \times \mathbf{B})$
3.2. Rippling mode:	$F_{adv} > (\mathbf{j} \times \mathbf{B})$
3.3. Tearing mode:	$(dB/dx)_{crit}$
4) Current Pinch Instabilities:	
4.1. Cylindrical pinch:	
4.1.1 Kink mode:	$B_{0\varphi}^2 \ln(L/a) > B_{0z}^2$
4.1.2 Sausage mode:	$B_{0\varphi}^2 > 2B_{0z}^2$
4.1.3 Helical/torsional mode:	$B_{0\varphi} > (2\pi a/L) B_{0z}$
4.2. Current sheet:	

Niestabilności MHD w pętlach koronalnych

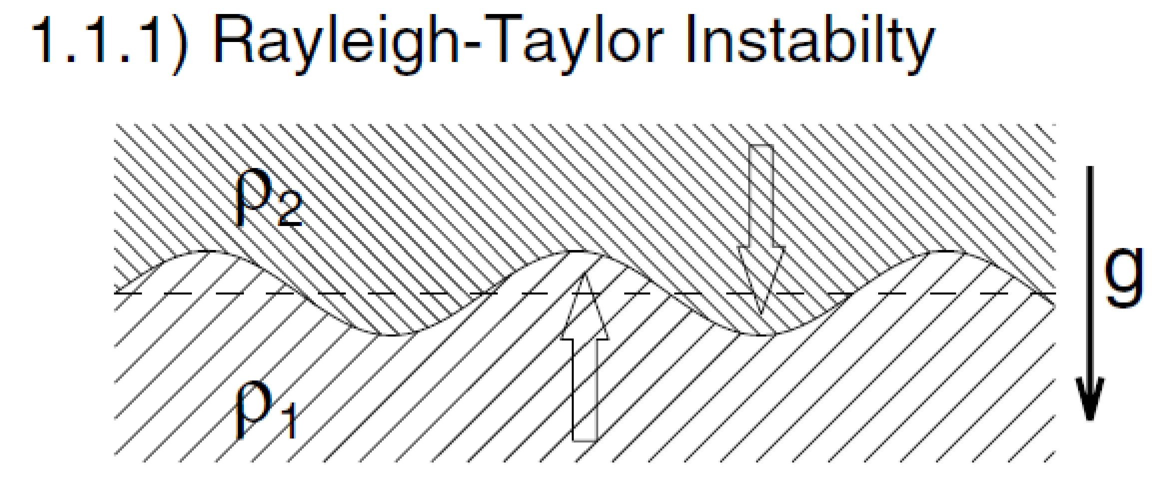

!!! => o niestabilnościach MHD w pętlach koronalnych proszę doczytać (w temacie wyjaśnień schematów prezentowanych na najbliższych slajdach) w *Aschwandenenie (Rozdział 6.3)*

Niestabilności MHD w pętlach koronalnych

1.1.2) Kruskal-Schwarzschild Instability

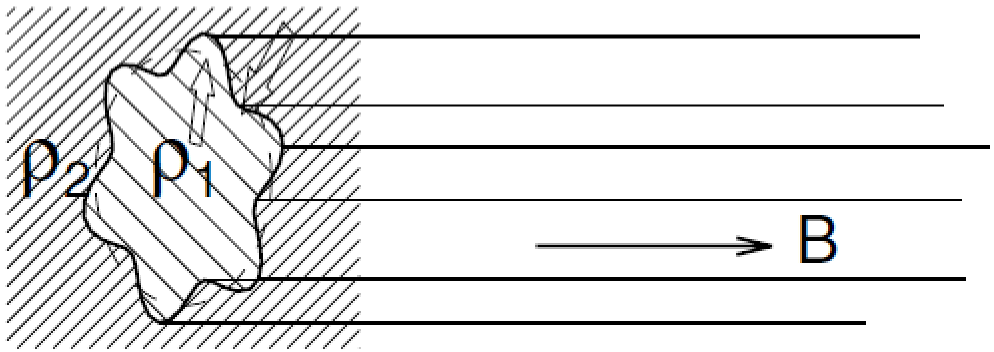

Niestabilności MHD w pętlach koronalnych

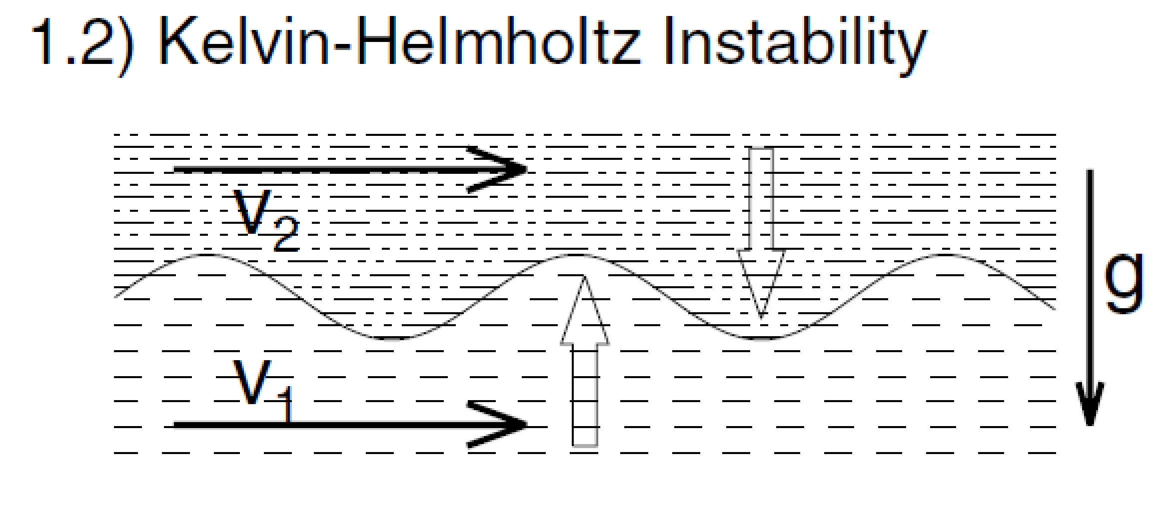

Niestabilności MHD w pętlach koronalnych

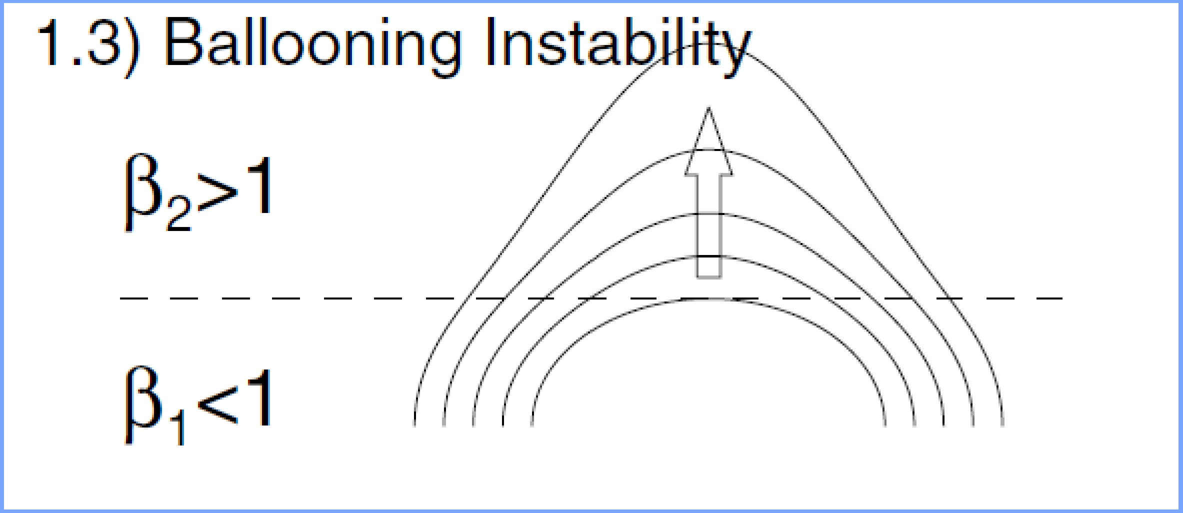

Niestabilności MHD w pętlach koronalnych

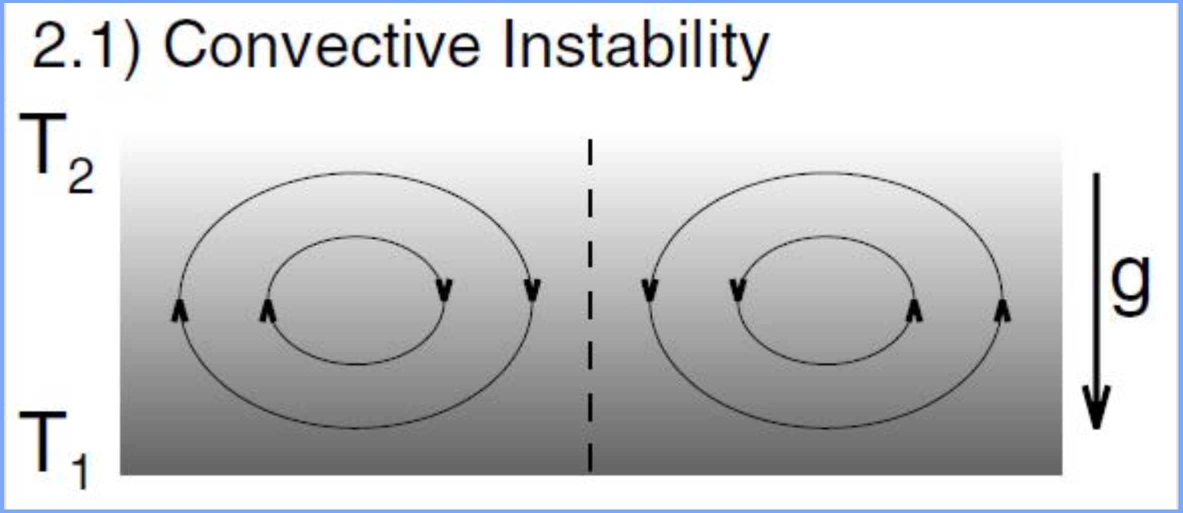

Niestabilności MHD w pętlach koronalnych

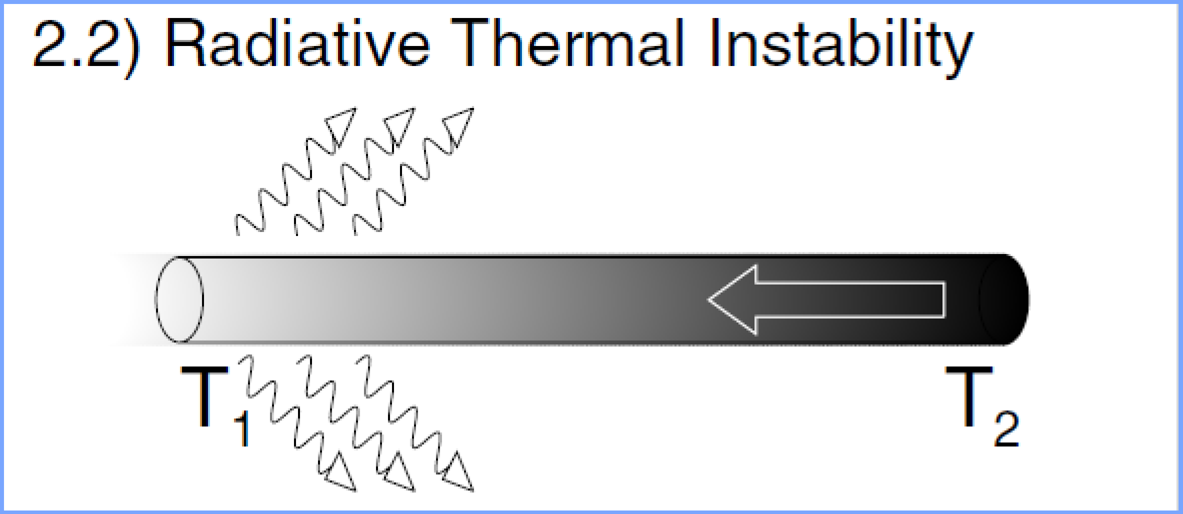

Niestabilności MHD w pętlach koronalnych

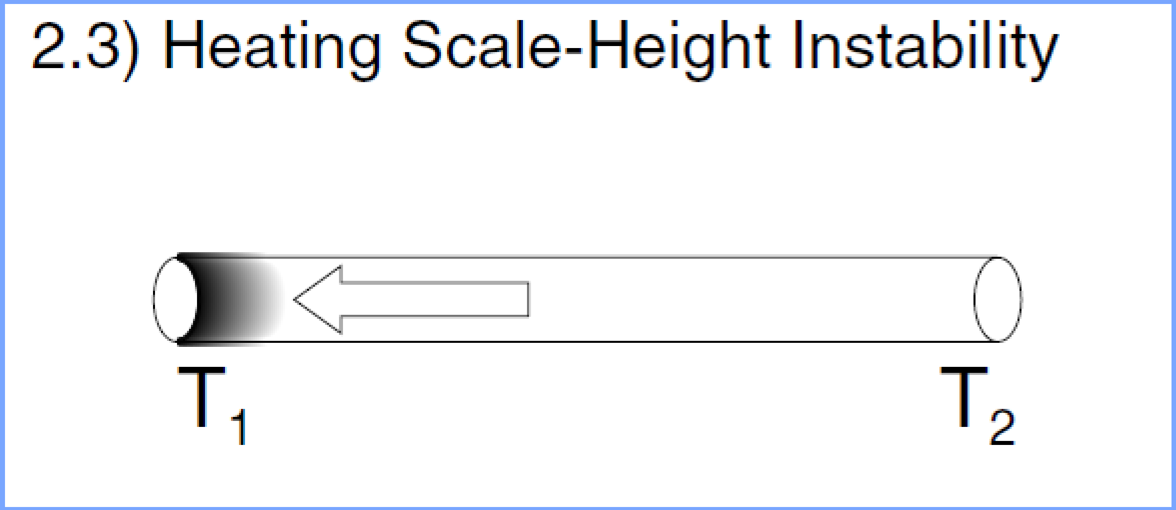

Niestabilności MHD w pętlach koronalnych

3.1) Gravitational Mode Instability

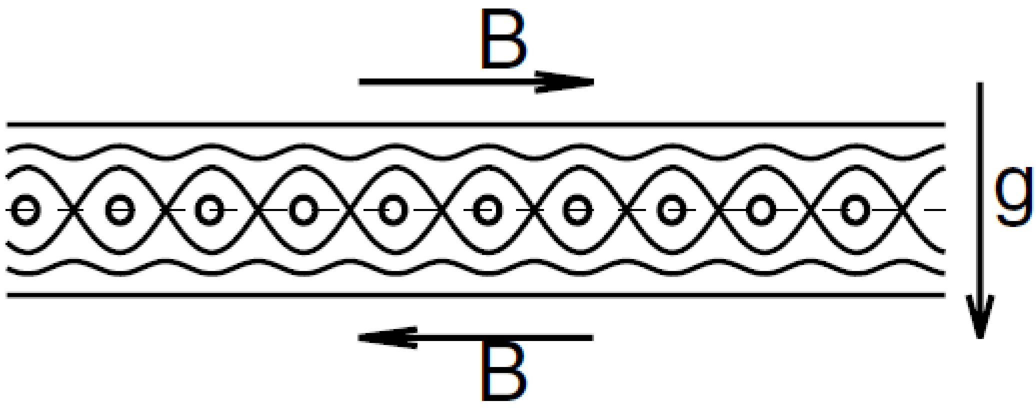

Niestabilności MHD w pętlach koronalnych

3.2) Rippling Mode Instability

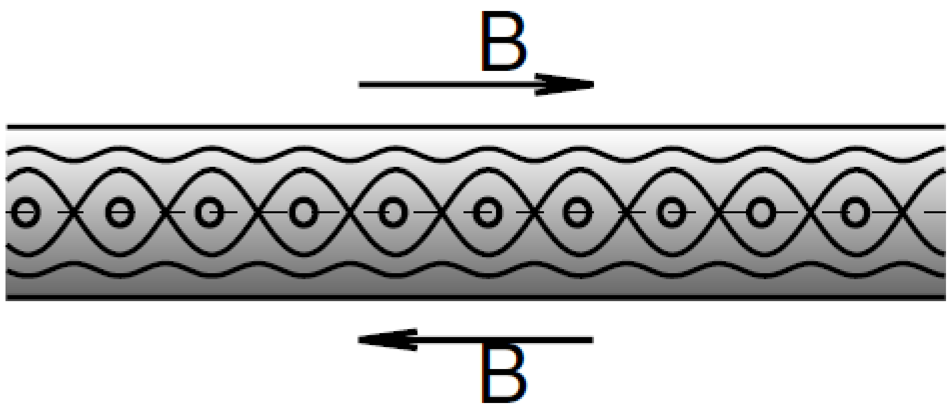

Niestabilności MHD w pętlach koronalnych

3.3) Tearing Mode Instability

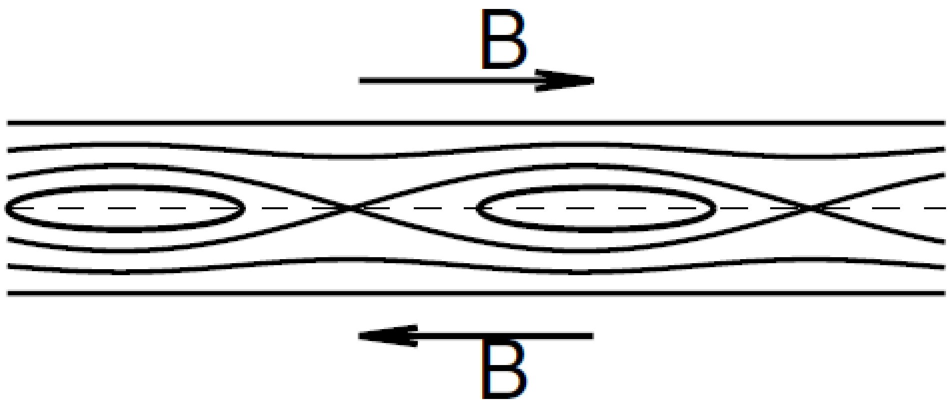

Niestabilności MHD w pętlach koronalnych

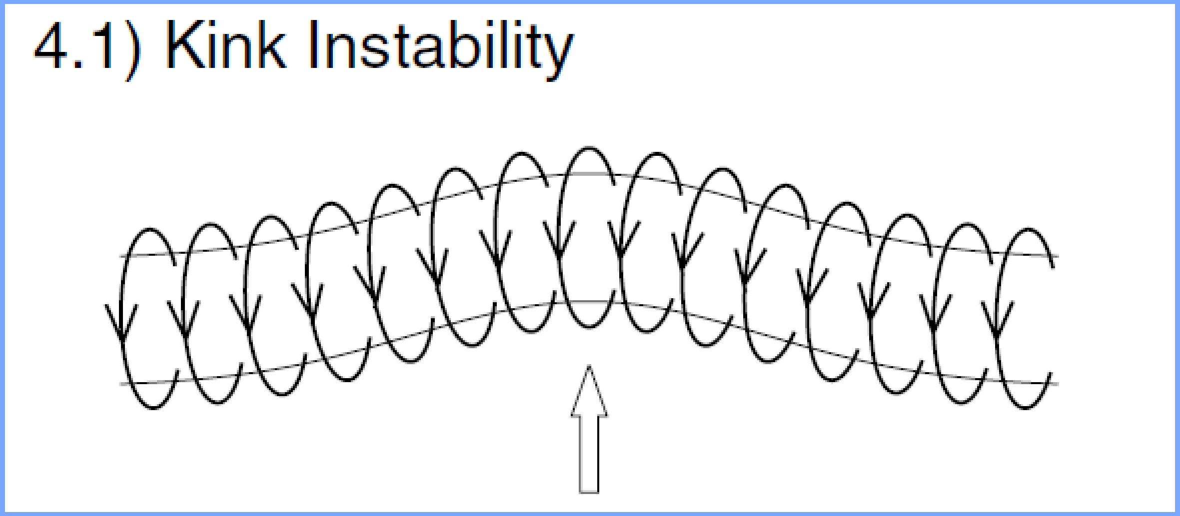

Niestabilności MHD w pętlach koronalnych

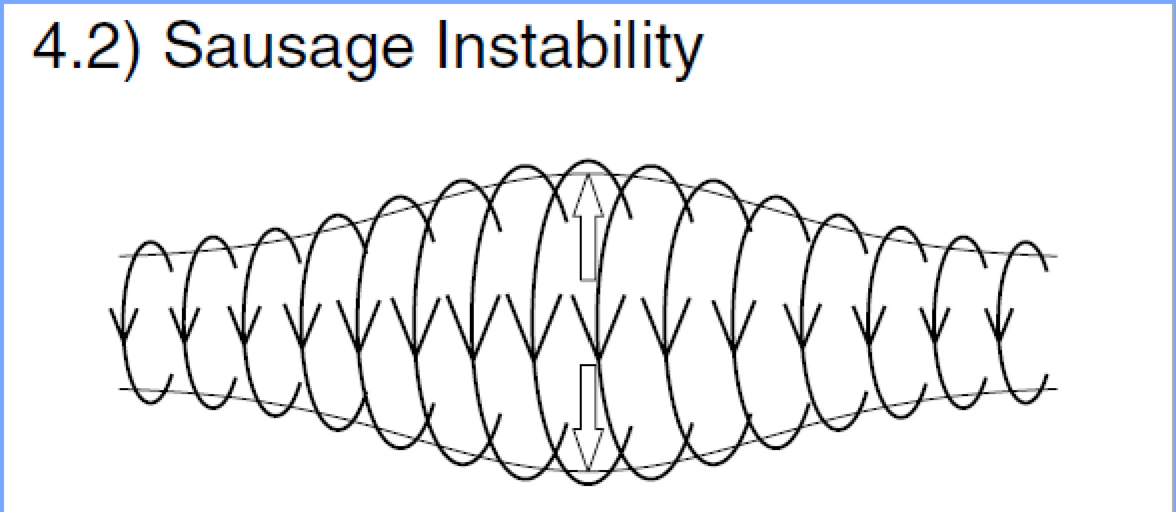

Niestabilności MHD w pętlach koronalnych

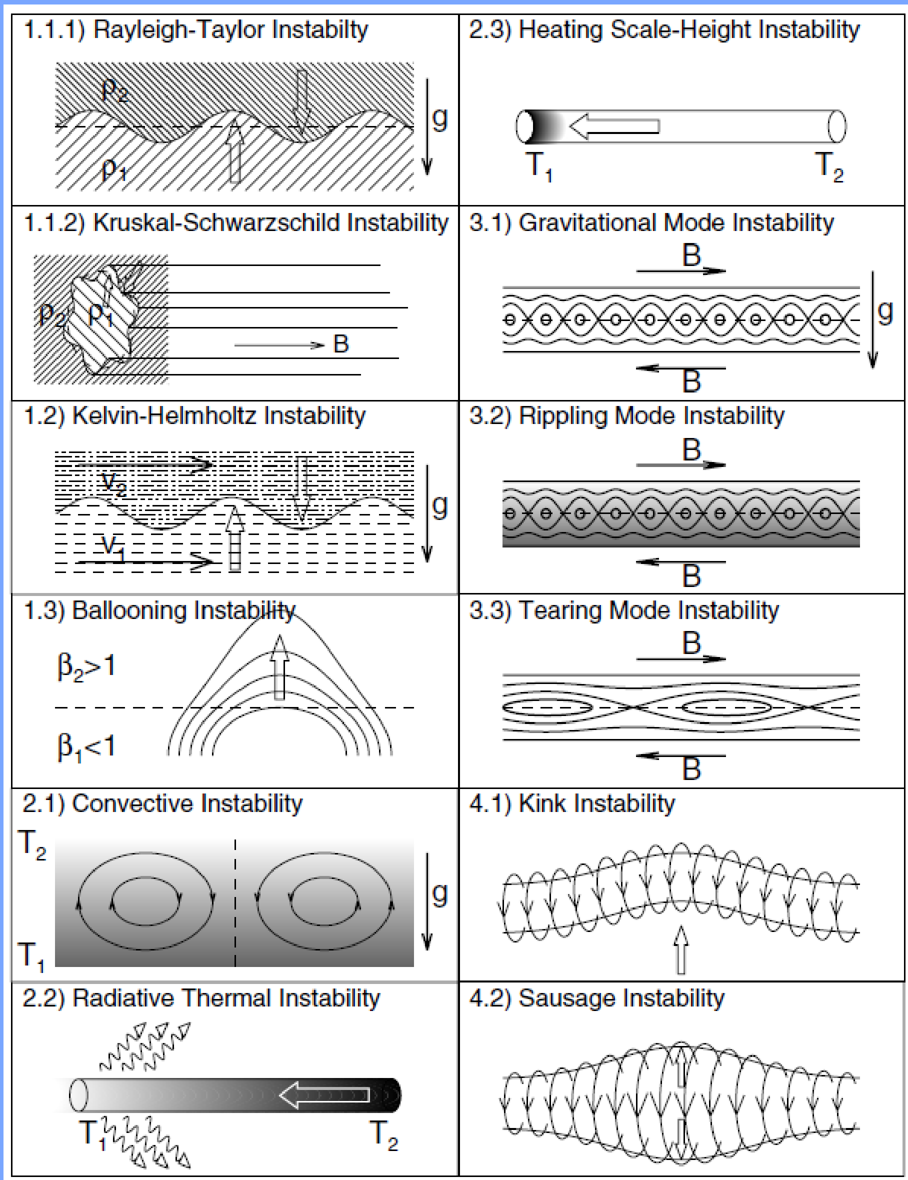

Table 6.1: Overview of HD and MHD instabilities in coronal loops.

Instability	Unstable condition
1) Interchange or Pressure-Driven Instabilities:	
1.1. Rayleigh–Taylor instability:	
1.1.1 Hydrodynamic:	$\mathbf{g} \cdot \nabla n_0 < 0$
1.1.2 Hydromagnetic (Kruskal–Schwarzschild):	$\mathbf{k} \cdot \mathbf{B} = 0$
1.1.3 Hydromagnetic (Parker instability):	$\mathbf{k} \cdot \mathbf{B} \neq 0$
1.2) Kelvin–Helmholtz instability:	
1.2.1 Hydromagnetic:	$v_1 > v_{A,2}$
1.3) Ballooning instability:	$\mathbf{j} \times \mathbf{B} > \rho \mathbf{g}$
2) Thermal Instabilities:	
2.1) Convective instabilities:	$(dT/dz)_{crit}$
2.2) Radiatively-driven thermal instabilities:	$\tau_{cond} > \tau_{rad}$
2.3) Heating-driven thermal instabilities:	$s_H/L < 1/3$
3) Resistive Instabilities:	
3.1. Gravitational mode:	$F_{grav} > (\mathbf{j} \times \mathbf{B})$
3.2. Rippling mode:	$F_{adv} > (\mathbf{j} \times \mathbf{B})$
3.3. Tearing mode:	$(dB/dx)_{crit}$
4) Current Pinch Instabilities:	
4.1. Cylindrical pinch:	
4.1.1 Kink mode:	$B_{0\varphi}^2 \ln(L/a) > B_{0z}^2$
4.1.2 Sausage mode:	$B_{0\varphi}^2 > 2B_{0z}^2$
4.1.3 Helical/torsional mode:	$B_{0\varphi} > (2\pi a/L)B_{0z}$
4.2. Current sheet:	

Aschwanden, „Physics of the Solar Corona”
=> Chapter 6.3

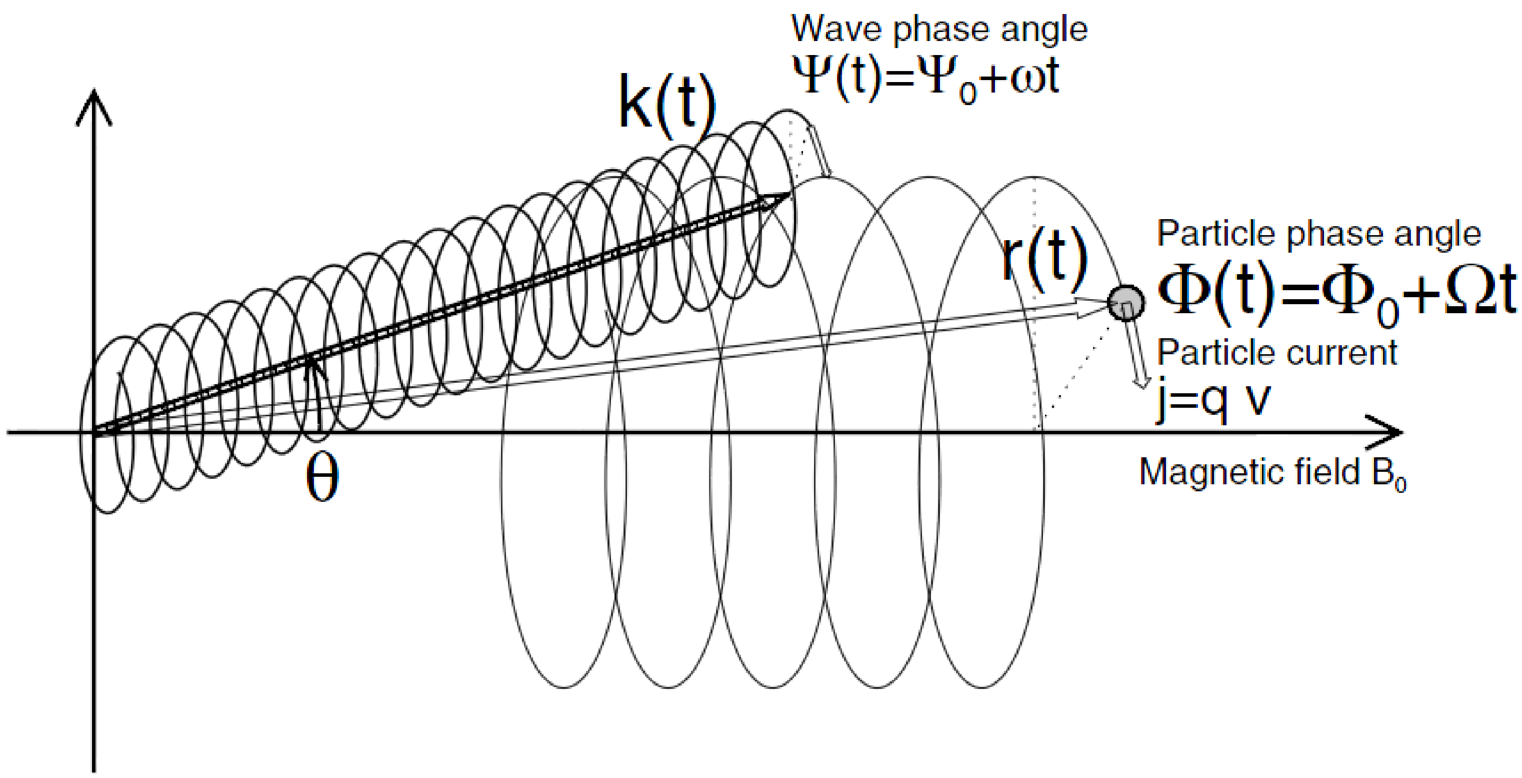

Figure 11.9: The wave-particle interaction between a wave with a propagation vector $\mathbf{k}(t)$ and a wave frequency ω, which has an angle θ to the magnetic field direction B_0, with a particle gyrating at position $\mathbf{r}(t)$ with gyrofrequency Ω around the guiding field B_0. The (azimuthal) phase angle of the wave vector is $\Psi(t)$ and of the particle is $\Phi(t)$.

Aschwanden, „Physics of the Solar Corona"

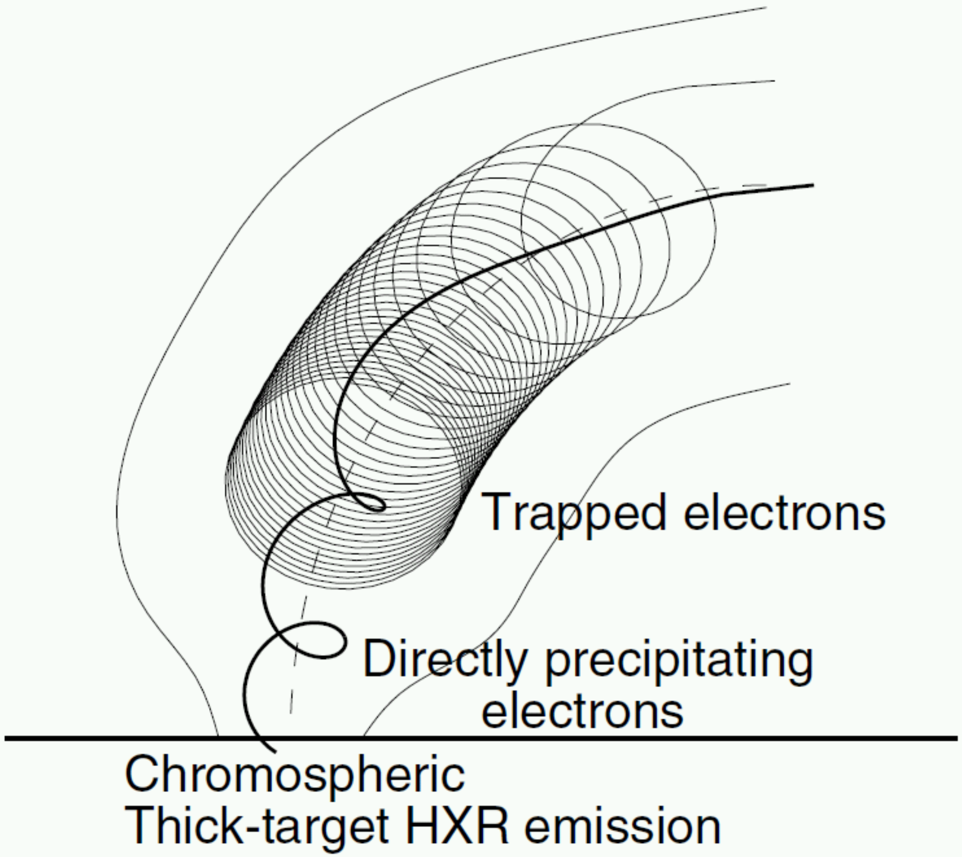

Figure 4. Electrons with small pitch angles precipitate directly, while electrons with large pitch angles become trapped and precipitate after many bounces and eventual scattering into the loss cone.

Modelowanie rozbłysków słonecznych

- podstawowe założenia

Modelowanie rozbłysków słonecznych

Model => zestaw parametrów

Wartości początkowe (wejściowe):

=> **Podstawowe parametry plazmy** *(skład, gęstość, temp., …)* - czyli odpowiedni model początkowy dla poszczególnych warstw

Co można otrzymać z numerycznych modelowań:

=> **Pole magnetyczne** [*korona, wnętrze Słońca, …*]

=> **Parametry fizyczne plazmy** [*skład plazmy, temperat., gęstość, miara emisji, …*]

=> **Zmiany MHD** [*przepływy, fale uderzeniowe, niestabilności, …*]

=> **Warstwa prądowa i obszar dyfuzyjny, przełączenia linii sił pola magnetycznego, prąd powrotny**

=> **Zmiany radiacyjne plazmy** [*poszczególne zakresy promieniowania elektromagne-tycznego, przy uwzględnieniu różnych mechanizmów emisji*]

=> **Wyrzuty plazmy (CME, SEP)**

Skutki rozbłysków słonecznych

oraz

ich wpływ na Ziemię i jej otoczenie

Skutki rozbłysków słonecznych oraz ich wpływ na Ziemię i jej otoczenie

Zakres wpływu rozbłysków:

=> korona, chromosfera

=> fotosfera (*WL-flares*)

=> zewnętrzna korona - przestrzeń międzyplanetarna - planety

=> heliosfera (cała)

Sposób oddziaływania rozbłysków:

=> promieniowanie elekrtomagnetyczne

=> cząstki (o prędkościach nierelatywistycznych i relatywistycznych)

=> przewodnictwo cieplne

=> fale uderzeniowe

=> zmiany pola magnetycznego

Skutki rozbłysków słonecznych oraz ich wpływ na Ziemię i jej otoczenie

Pogoda kosmiczna [*space weather*]

http://www.swpc.noaa.gov/

Skutki rozbłysków słonecznych oraz ich wpływ na Ziemię i jej otoczenie

Pogoda kosmiczna [*space weather*]

http://www.swpc.noaa.gov/

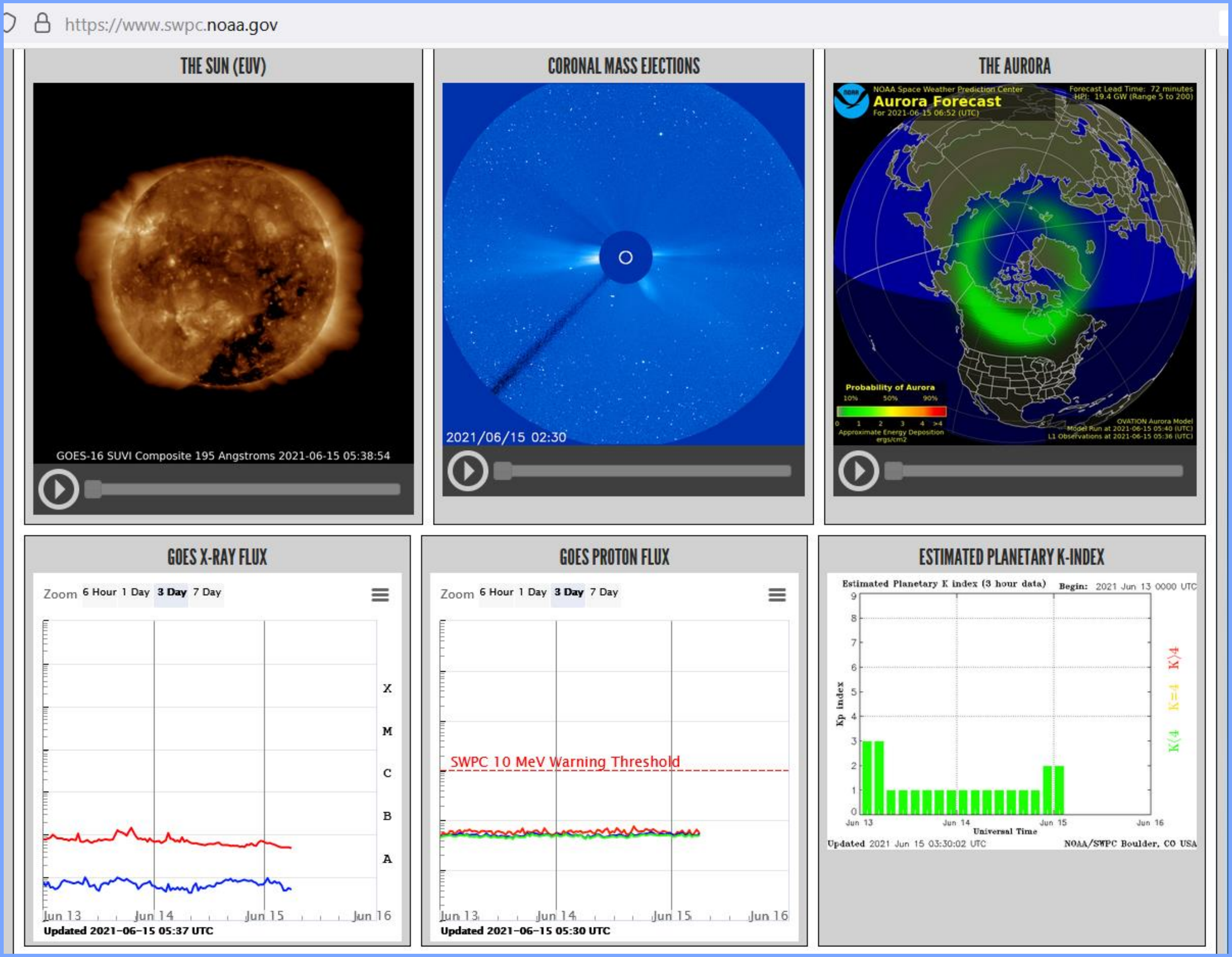

Skutki rozbłysków słonecznych oraz ich wpływ na Ziemię i jej otoczenie

Pogoda kosmiczna [*space weather*]

GOES X-RAY FLUX

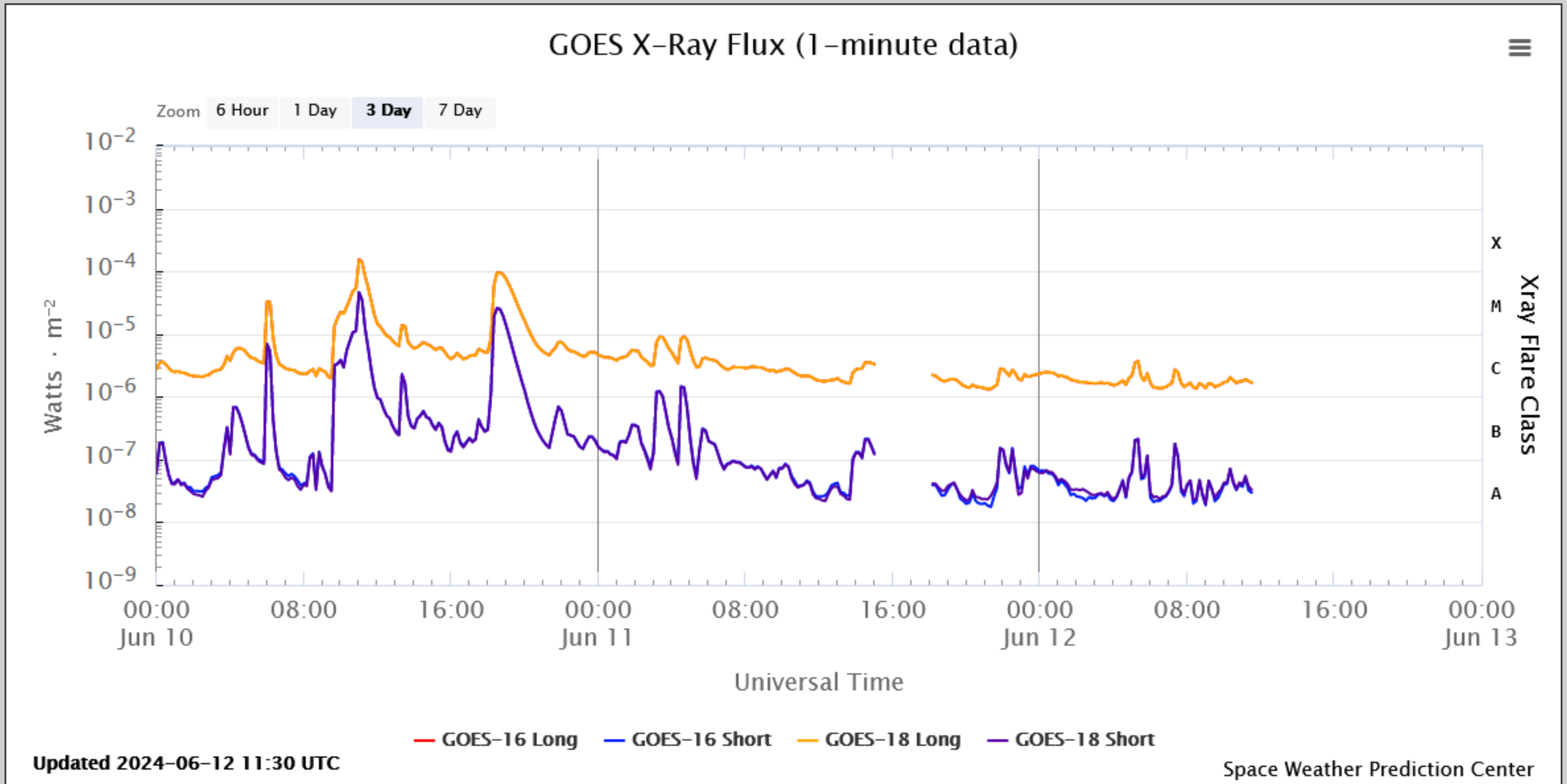

GOES-16 LATEST X-RAY EVENT 1-8Å			
Current	12 Jun 2024 11:29:00 GMT	C1.6	Ratio 0.018
Beginning	12 Jun 2024 07:23:00 GMT	C1.5	
Maximum	12 Jun 2024 07:28:00 GMT	C2.7	Integrated flux: 1.8e-3 J m^{-2}
End	12 Jun 2024 07:36:00 GMT	C1.9	

https://www.swpc.noaa.gov/products/goes-x-ray-flux => SXR (*GOES*)

Skutki rozbłysków słonecznych oraz ich wpływ na Ziemię i jej otoczenie

Pogoda kosmiczna [*space weather*]

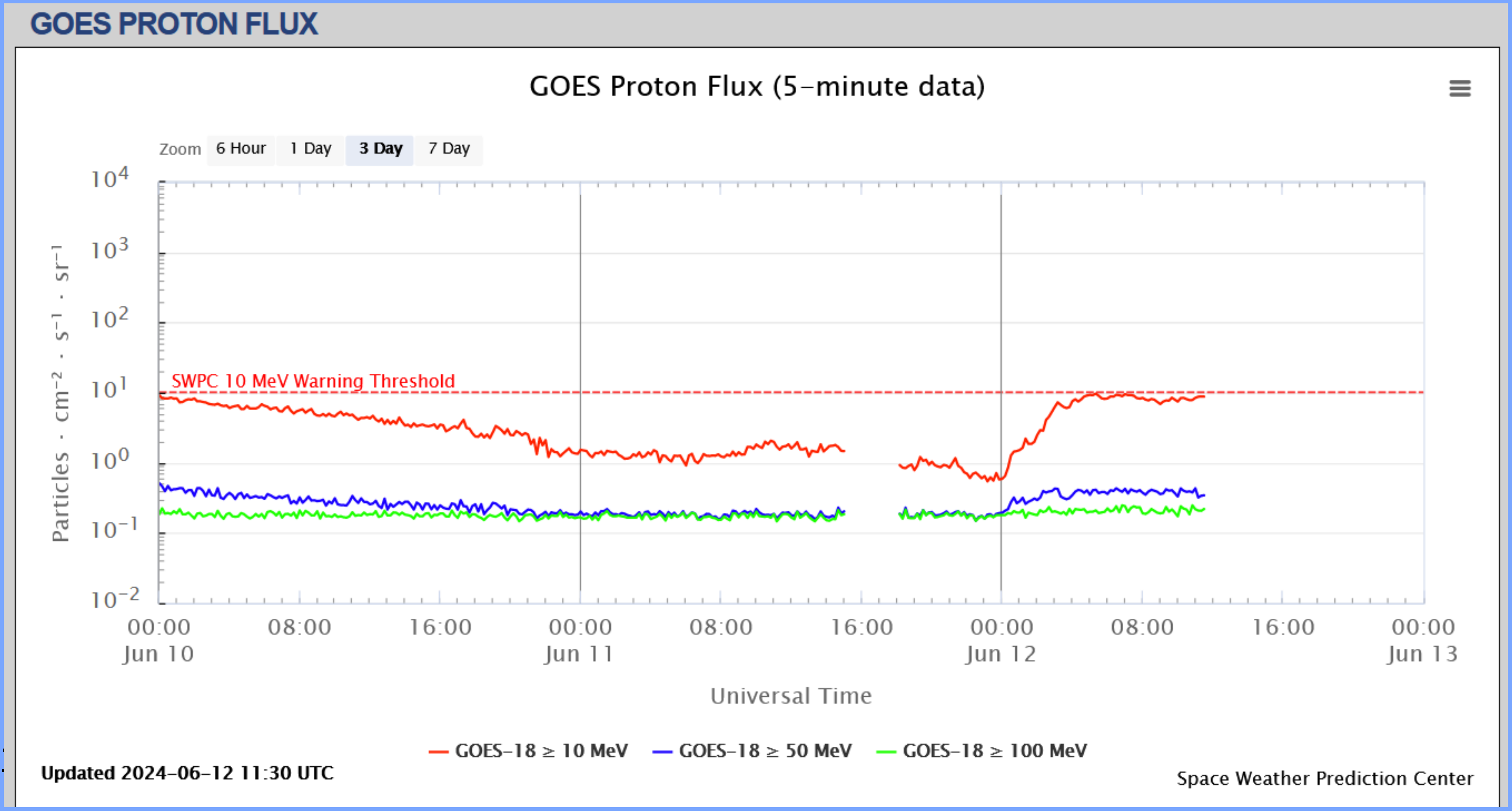

https://www.swpc.noaa.gov/products/goes-proton-flux => Protons (*GOES*)

Skutki rozbłysków słonecznych oraz ich wpływ na Ziemię i jej otoczenie

Pogoda kosmiczna [*space weather*]

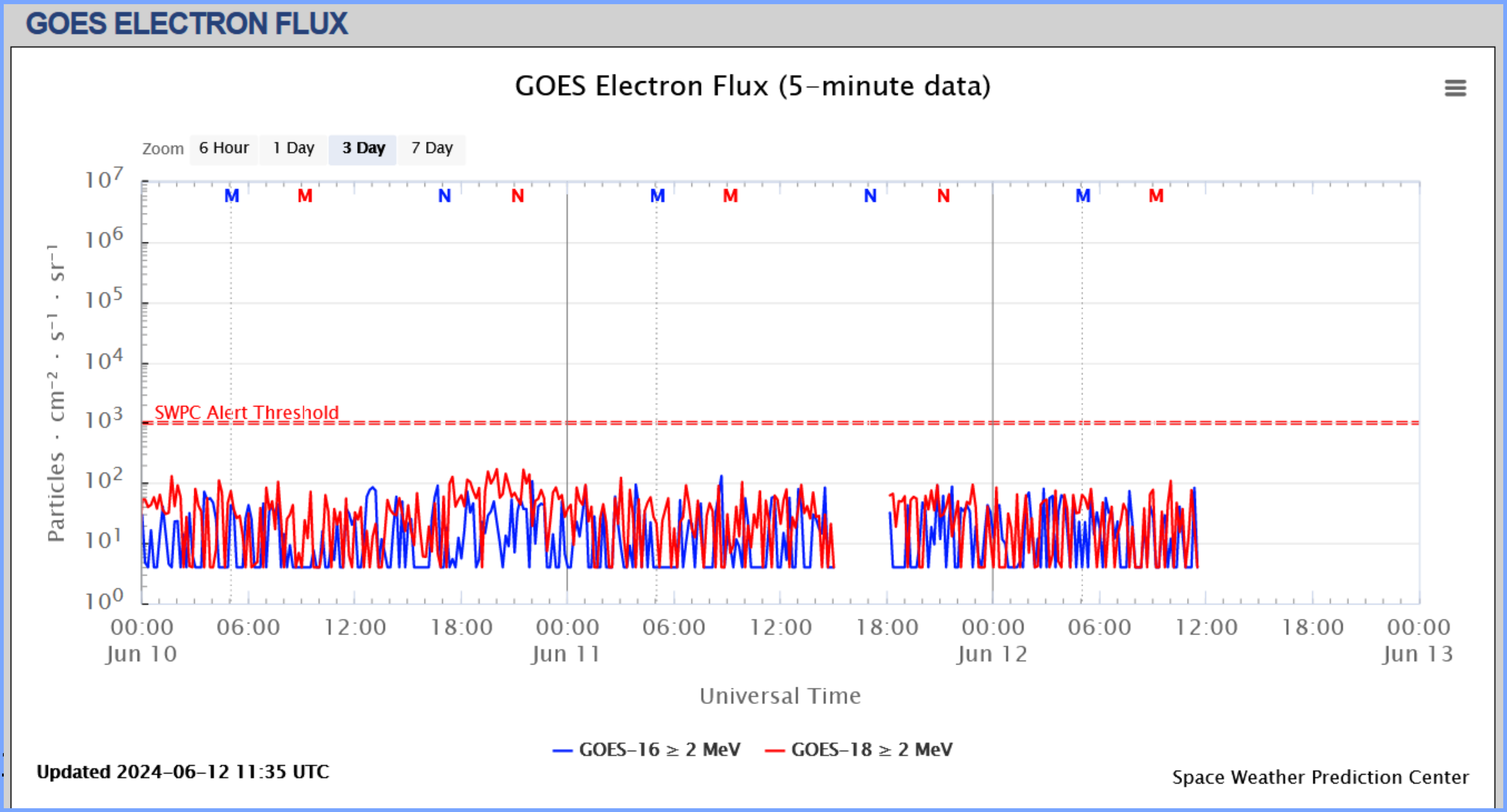

https://www.swpc.noaa.gov/products/goes-electron-flux => Electrons (*GOES*)

Skutki rozbłysków słonecznych oraz ich wpływ na Ziemię i jej otoczenie

Pogoda kosmiczna [*space weather*]

K-index (Juliusz Bartels, 1938 r.) określa zaburzenie horyzontalnej (poziomej) składowej pola magnetycznego Ziemi. K-index oznaczany jest wartościami z zakresu: 0-9, gdzie 1 to niezaburzone pole, a 5 lub większa wartość wskazuje na występowanie geomagnetycznej burzy. [*Nazwa (K) pochodzi od niemieckiego słowa Kennziffer, co oznacza „charakterystyczną cyfrę”.*]

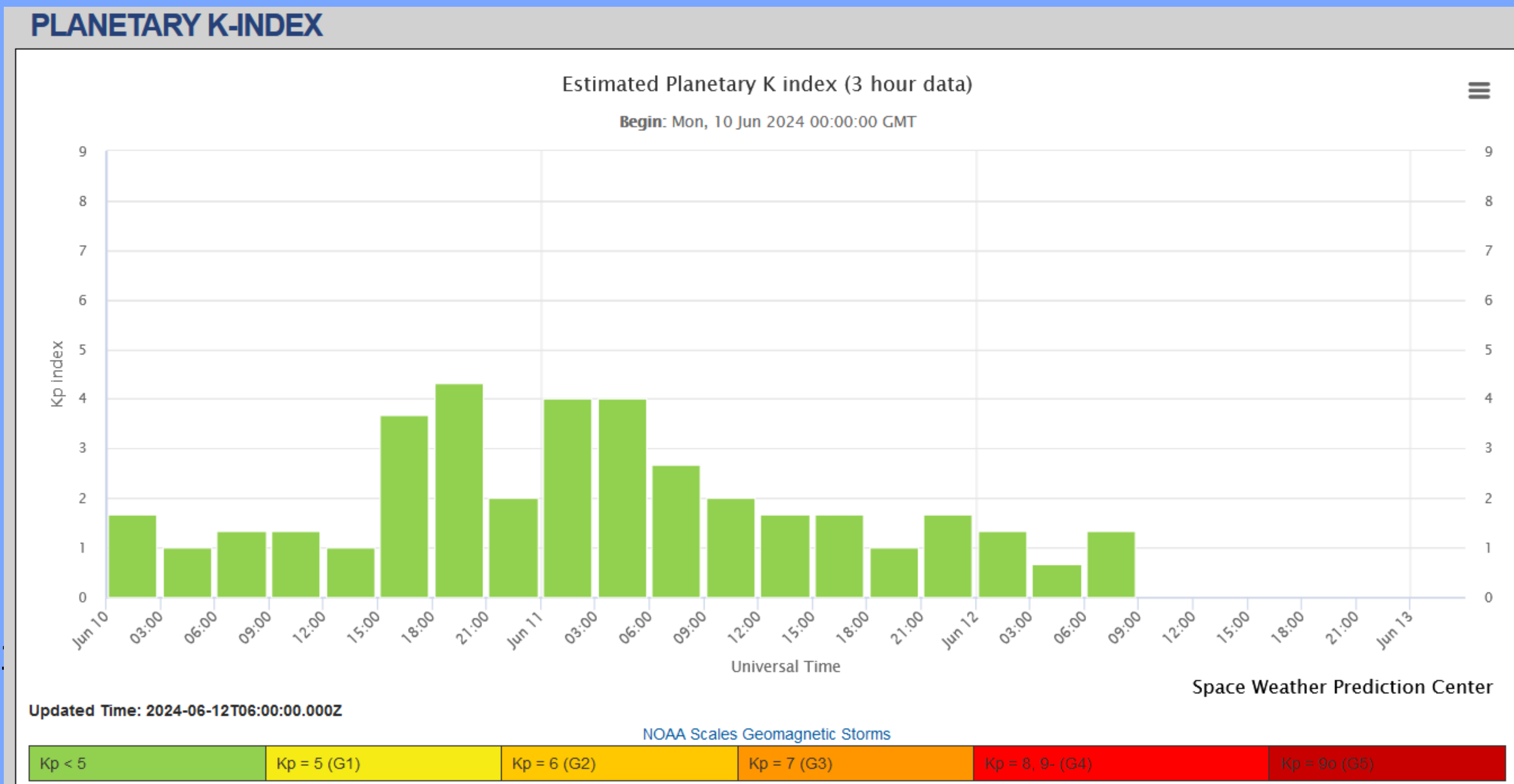

https://www.swpc.noaa.gov/products/planetary-k-index => K-Index (*GOES*)

K-index 11 maja 2024 roku osiągnął kilkukrotnie maksymalną wartość (w 9-cio stopniowej skali), czemu towarzyszyły widoczne na terenie Polski zorze polarne - także w okolicach zenitalnych.

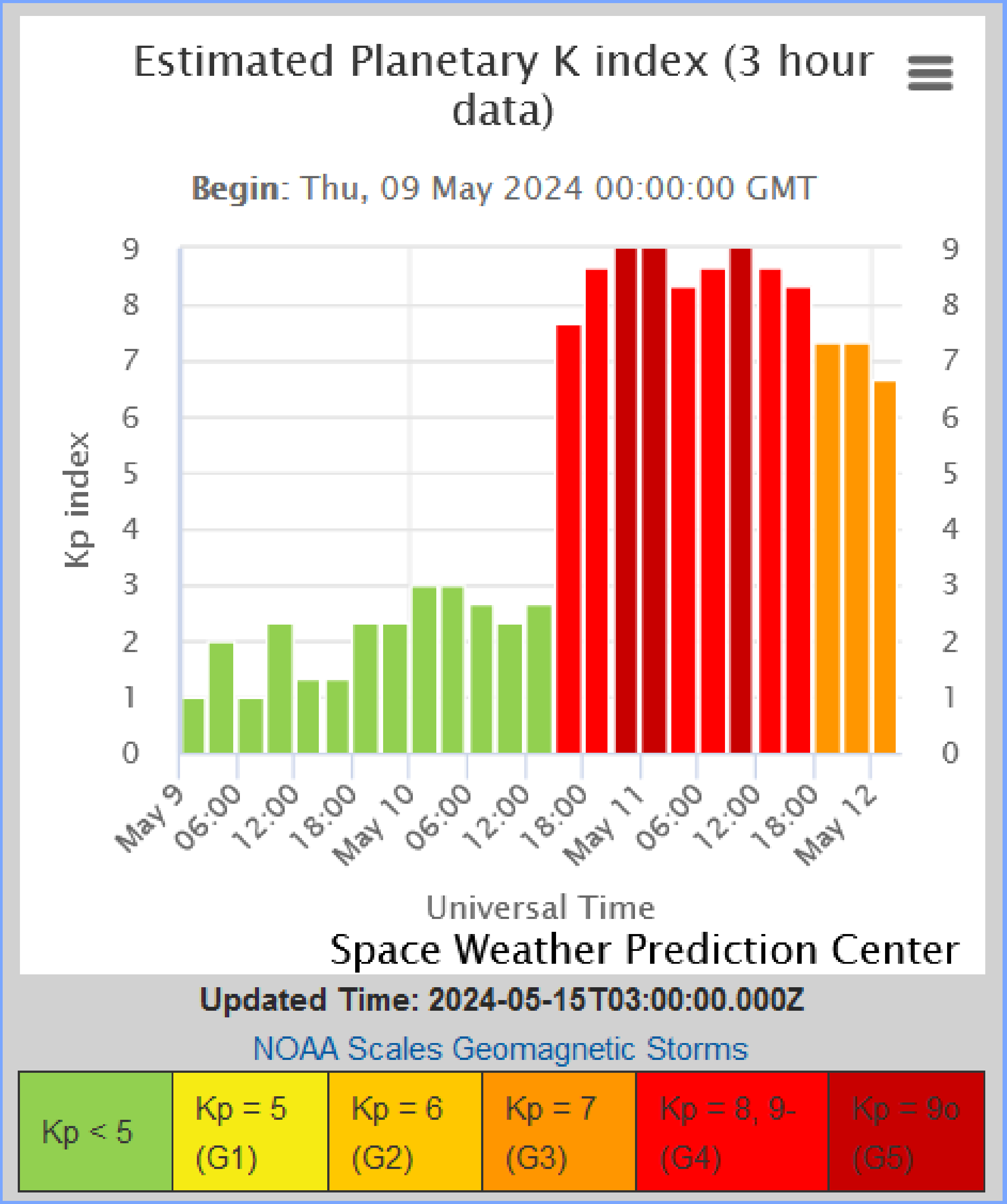

Skutki rozbłysków słonecznych oraz ich wpływ na Ziemię i jej otoczenie

Strumienie protonów różnego pochodzenia docierające do Ziemi

Table 7.1 Energy and flux of protons arriving at Earth[a]

Source	Energy (MeV)	Flux (protons m^{-2} s^{-1})
Cosmic rays	1,000	6×10^{2}
Coronal mass ejections	10	3×10^{8}
Solar flares	10	1×10^{7}
Solar wind	0.001	5×10^{12}

[a] An energy of 1 MeV $= 10^{6}$ eV $= 1.6 \times 10^{-6}$ erg $= 1.6 \times 10^{-13}$ J

Lang, „The Sun from space”

Skutki rozbłysków słonecznych oraz ich wpływ na Ziemię i jej otoczenie

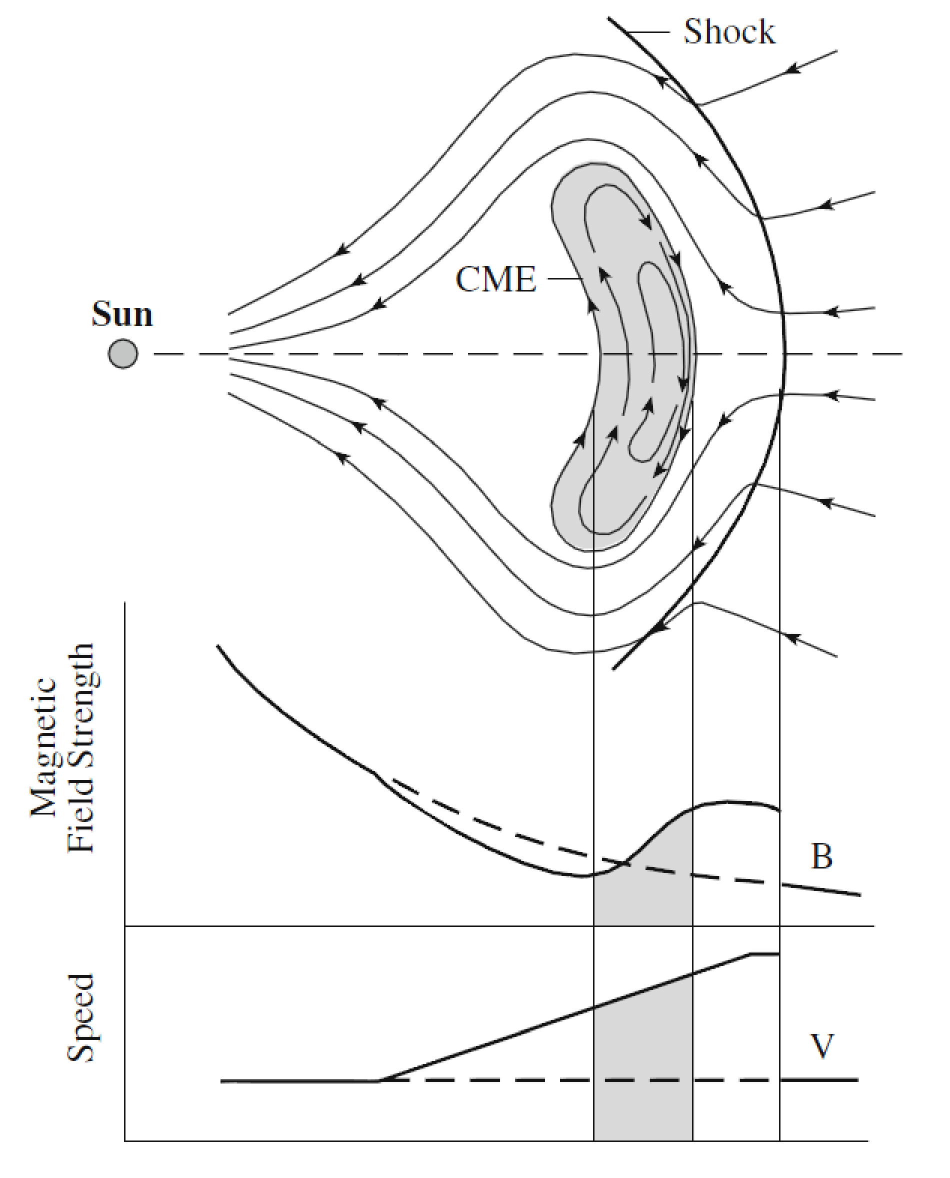

Rozchodzenie się zaburzenia (CME) w przestrzeni międzyplanetarnej.

Zmiany pola magnetycznego

Zmiany prędkości wiatru słonecznego

Lang, „The Sun from space”

Skutki rozbłysków słonecznych oraz ich wpływ na Ziemię i jej otoczenie

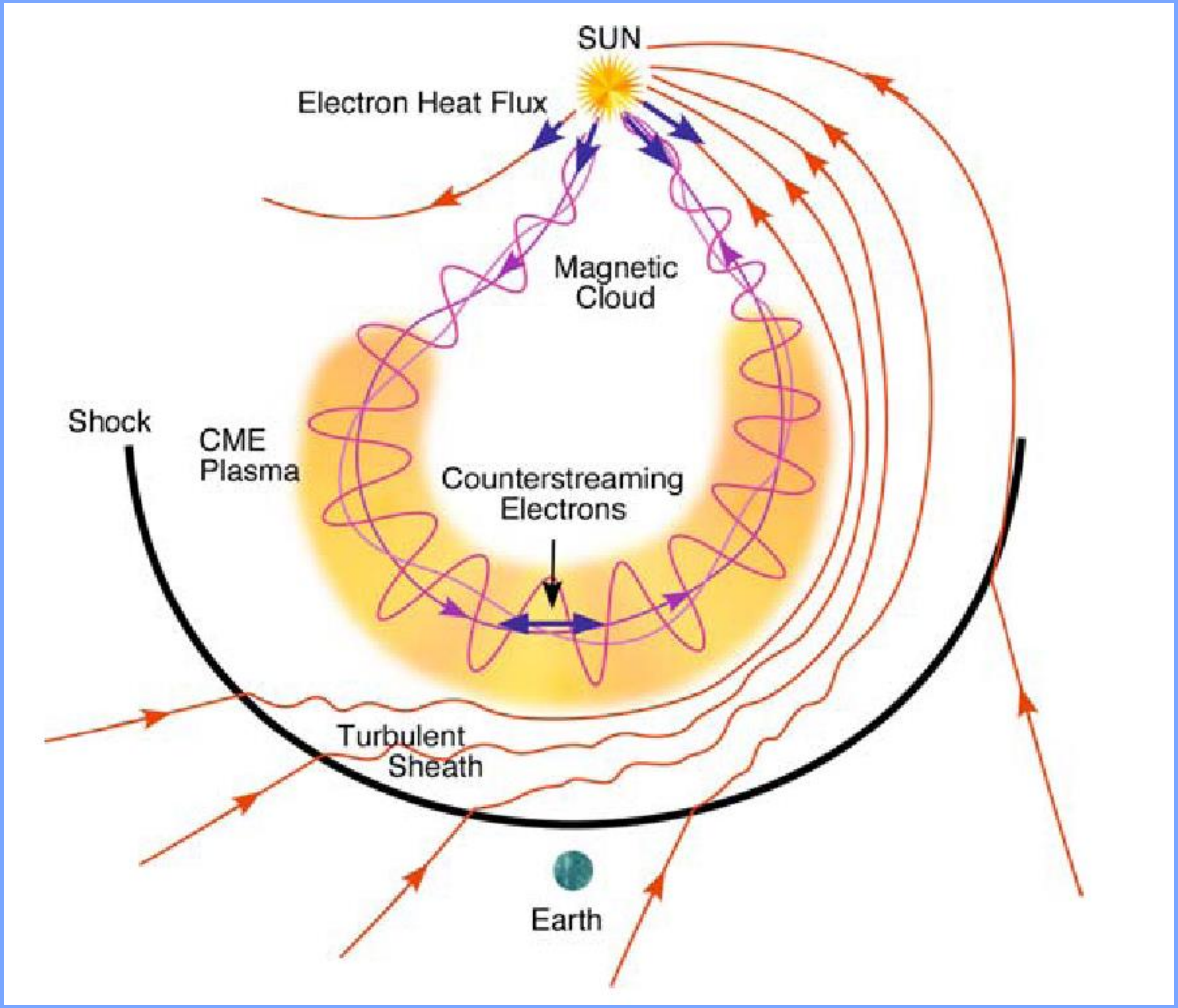

Struktura magnetyczna zaburzenia typu CME w momencie docierania do Ziemi.

Lang, „The Sun from space"

Skutki rozbłysków słonecznych oraz ich wpływ na Ziemię i jej otoczenie

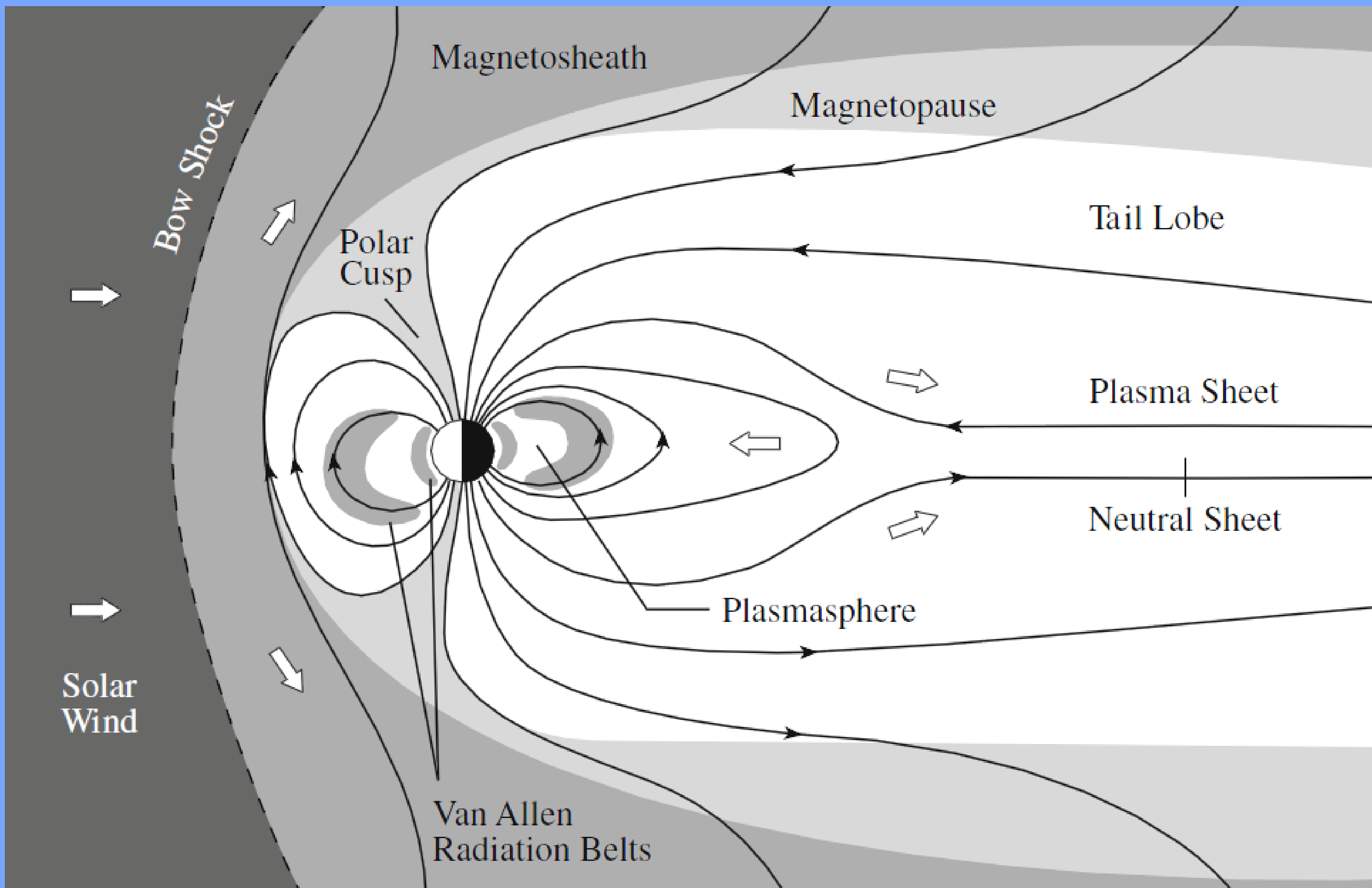

Lang, „The Sun from space"

Skutki rozbłysków słonecznych oraz ich wpływ na Ziemię i jej otoczenie

Zamknięcie linii sił pola magnetycznego w warstwie neutralnej

strzałki swobodne – oznaczają kierunek wiatru słonecznego
strzałki na liniach – oznaczają kierunek międzyplanetarnego i ziemskiego pola magnetycznego

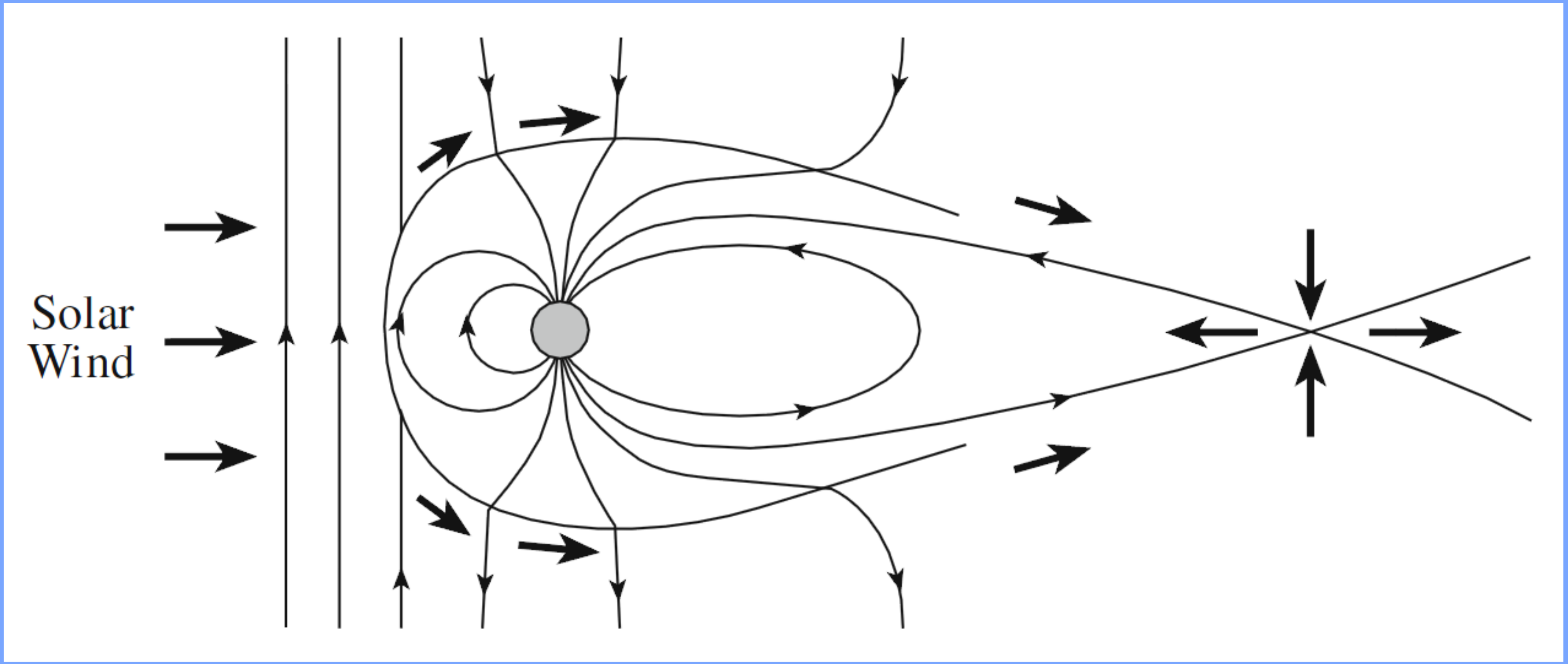

Lang, „The Sun from space”

Skutki rozbłysków słonecznych oraz ich wpływ na Ziemię i jej otoczenie

Korelacja liczby Wolfa z poszczególnymi składowymi (H, Z, D) pola magnetycznego.

H – składowa pozioma (horyzontalna)
Z – składowa pionowa
D – deklinacja

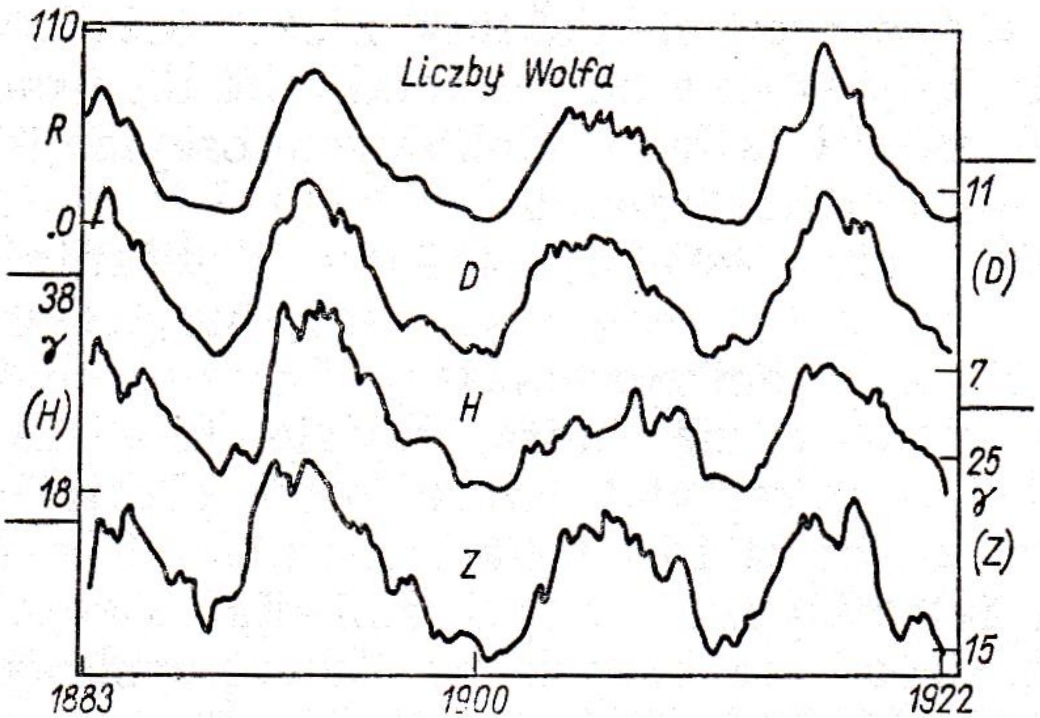

42. Liczby Wolfa i składowe magnetyczne *D*, *Z* i *H* (wg E. Stenza i M. Mackiewicz)

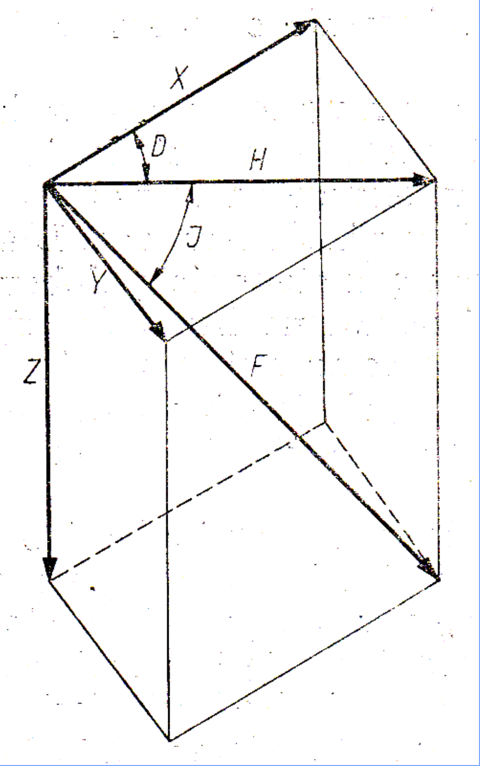

Mergentaler, „Słońce-Ziemia”

Skutki rozbłysków słonecznych oraz ich wpływ na Ziemię i jej otoczenie

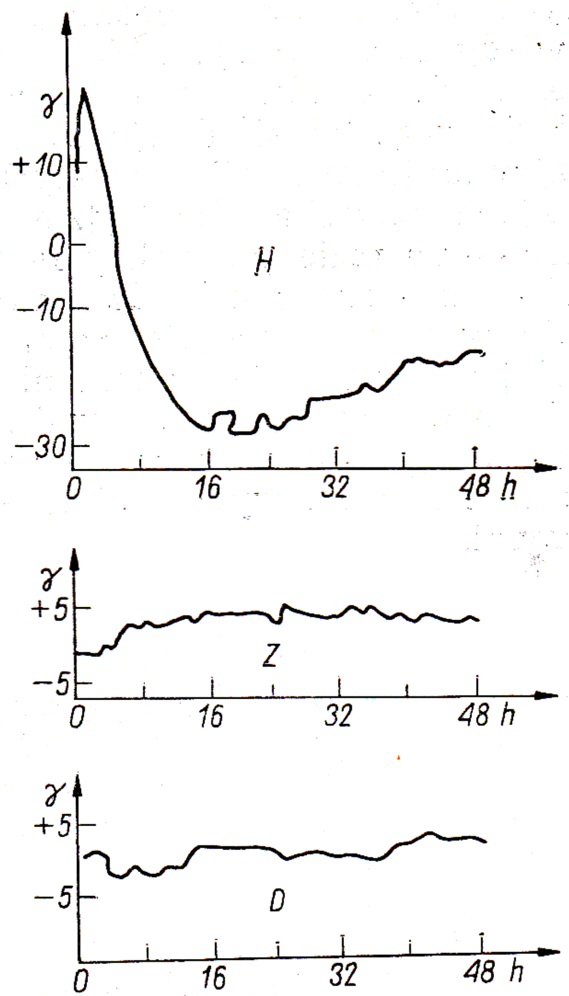

49. Obserwowane (uśrednione z trzech stacji) zmiany składowych *H*, *Z* i *D* w czasie burzy magnetycznej (wg E. Stenza i M. Mackiewicz)

Zmiany pola magnetycznego (składowych H, Z, D) podczas burzy magnetycznej.

Mergentaler, „Słońce-Ziemia”

Skutki rozbłysków słonecznych oraz ich wpływ na Ziemię i jej otoczenie

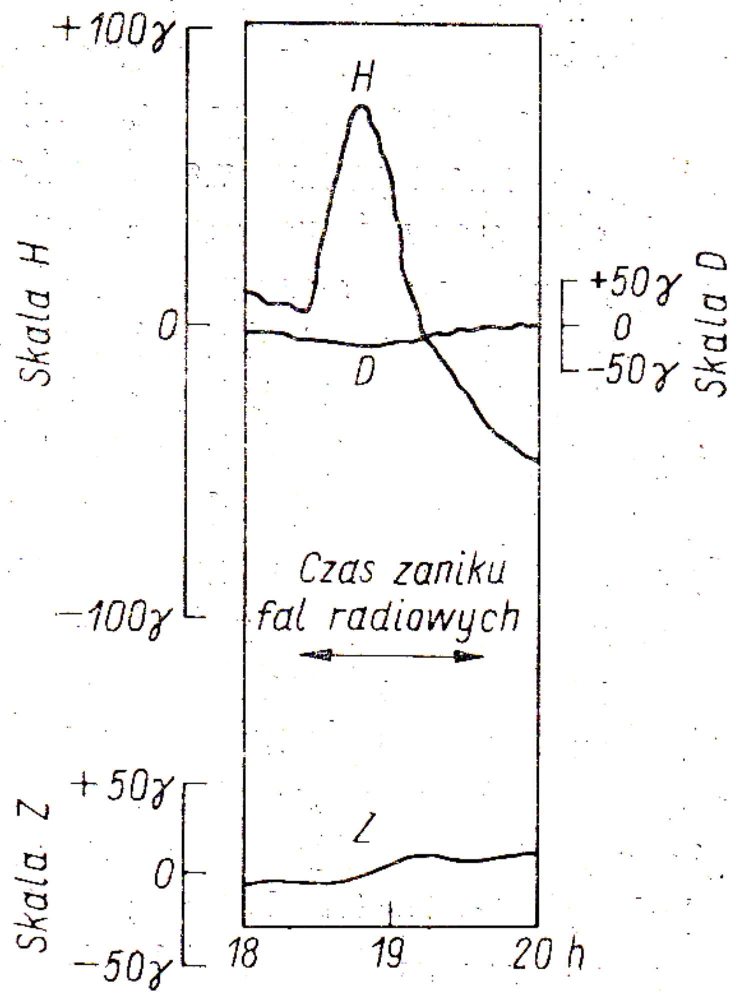

43. Zanik fal radiowych i *crochet* magnetyczny z 25 VIII 1936 r. (wg E. Stenza i M. Mackiewicz)

Crochet magnetyczny

[crochet(fr.) = hak]

Mergentaler, „Słońce-Ziemia”

Skutki rozbłysków słonecznych oraz ich wpływ na Ziemię i jej otoczenie

„Zasięg” wnikania fotonów (w atmosferę) w zależności od ich energii (długości fali).

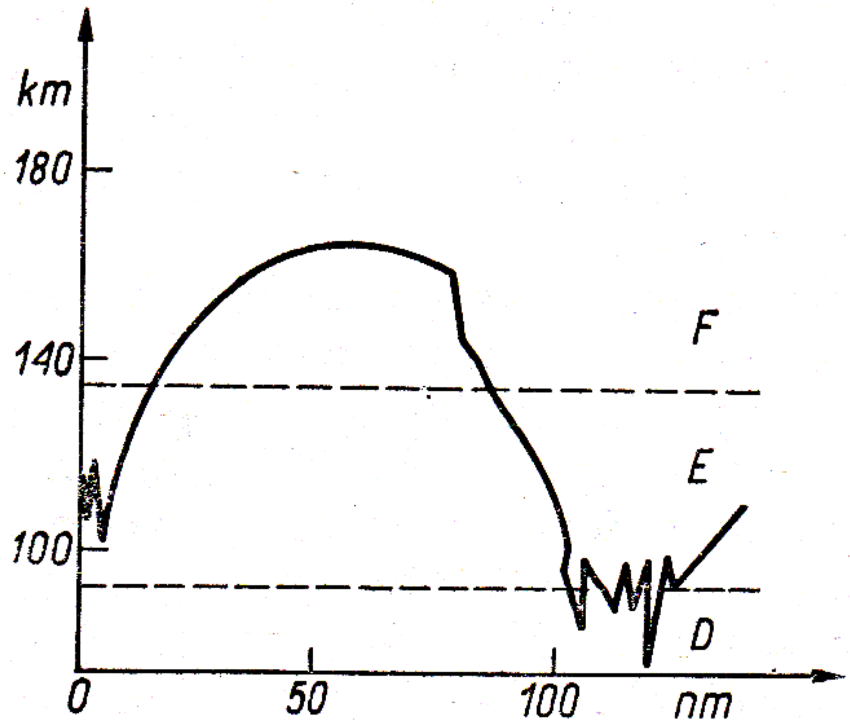

38. Głębokość wnikania w atmosferę promieniowania o różnych długościach fali (zaznaczono też wysokości warstw *D*, *E* i *F* jonosfery)

Mergentaler, „Słońce-Ziemia”

Skutki rozbłysków słonecznych oraz ich wpływ na Ziemię i jej otoczenie

„Zasięg” wnikania protonów (w atmosferę) i elektronów w zależności od ich energii.

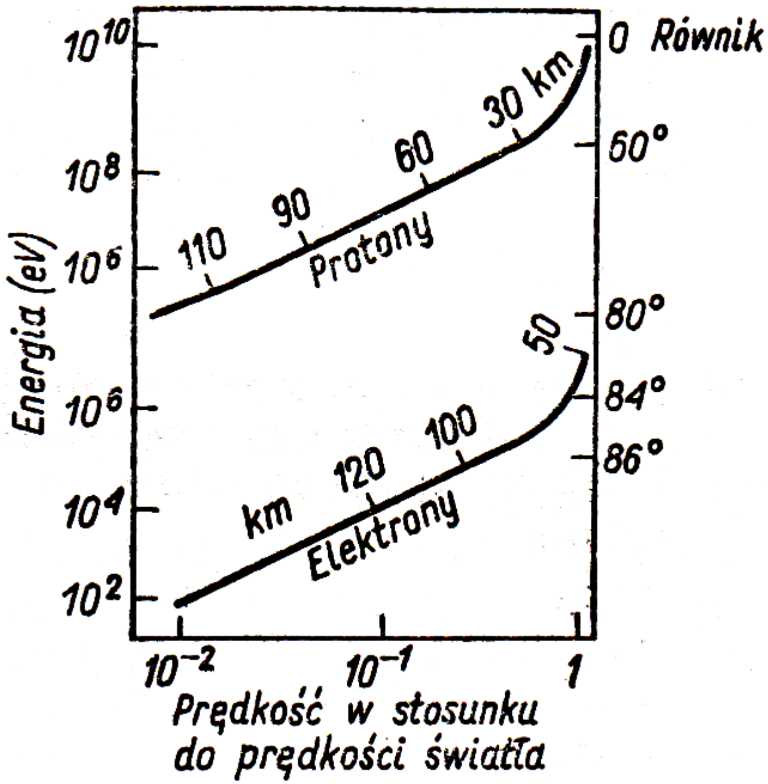

40. Przenikanie elektronów i protonów w atmosferę ziemską. Liczby na krzywych oznaczają wysokość nad powierzchnią Ziemi, do której docierają protony lub elektrony o danych energiach (wg J. R. Ratcliffa)

Mergentaler, „Słońce-Ziemia”

Skutki rozbłysków słonecznych oraz ich wpływ na Ziemię i jej otoczenie

Zmiany temperatury i ciśnienia z wysokością w atmosferze Ziemi

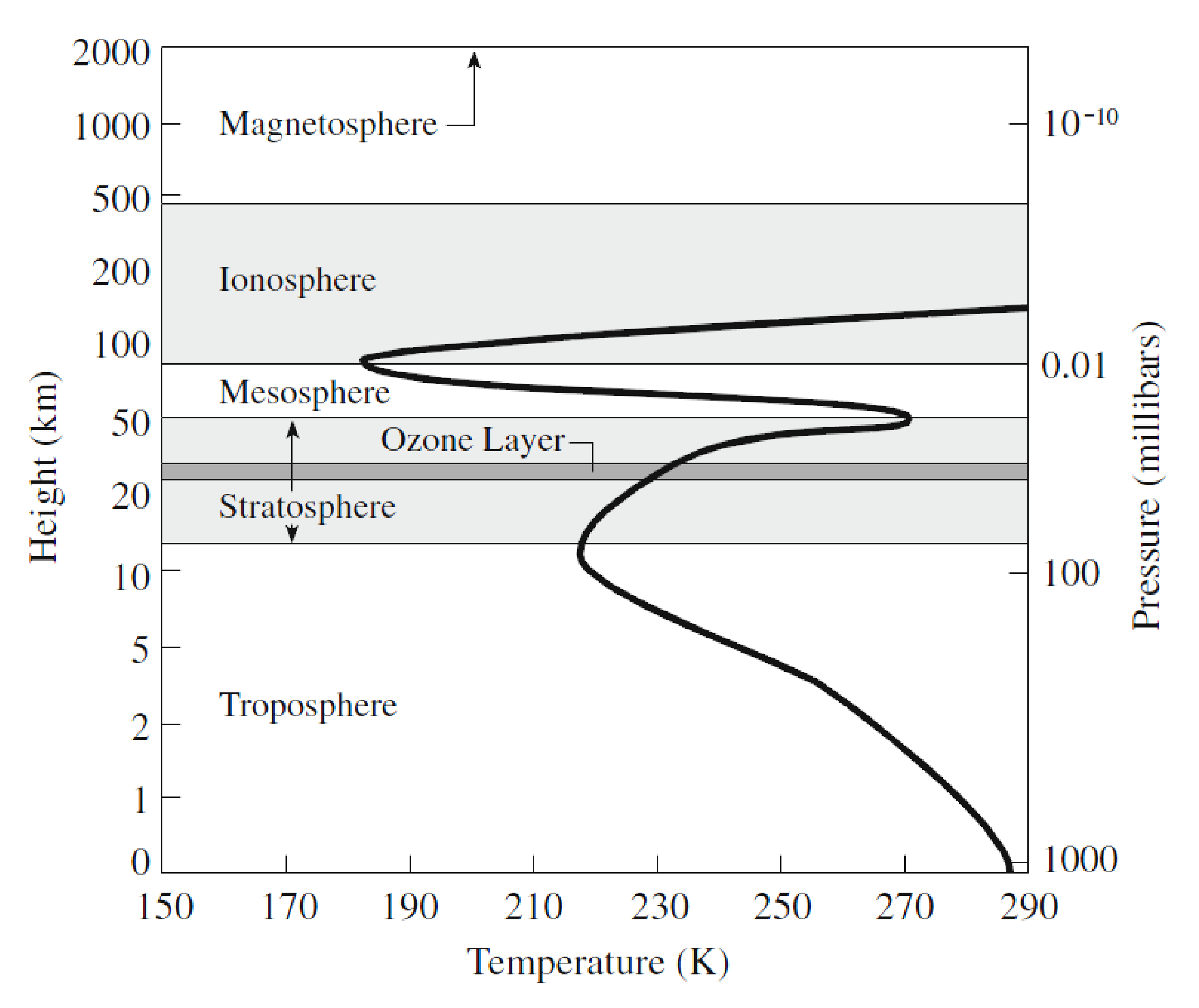

Lang, „The Sun from space”

Skutki rozbłysków słonecznych oraz ich wpływ na Ziemię i jej otoczenie

Zmiany grzania górnej atmosfery (min-max aktywności słonecznej)

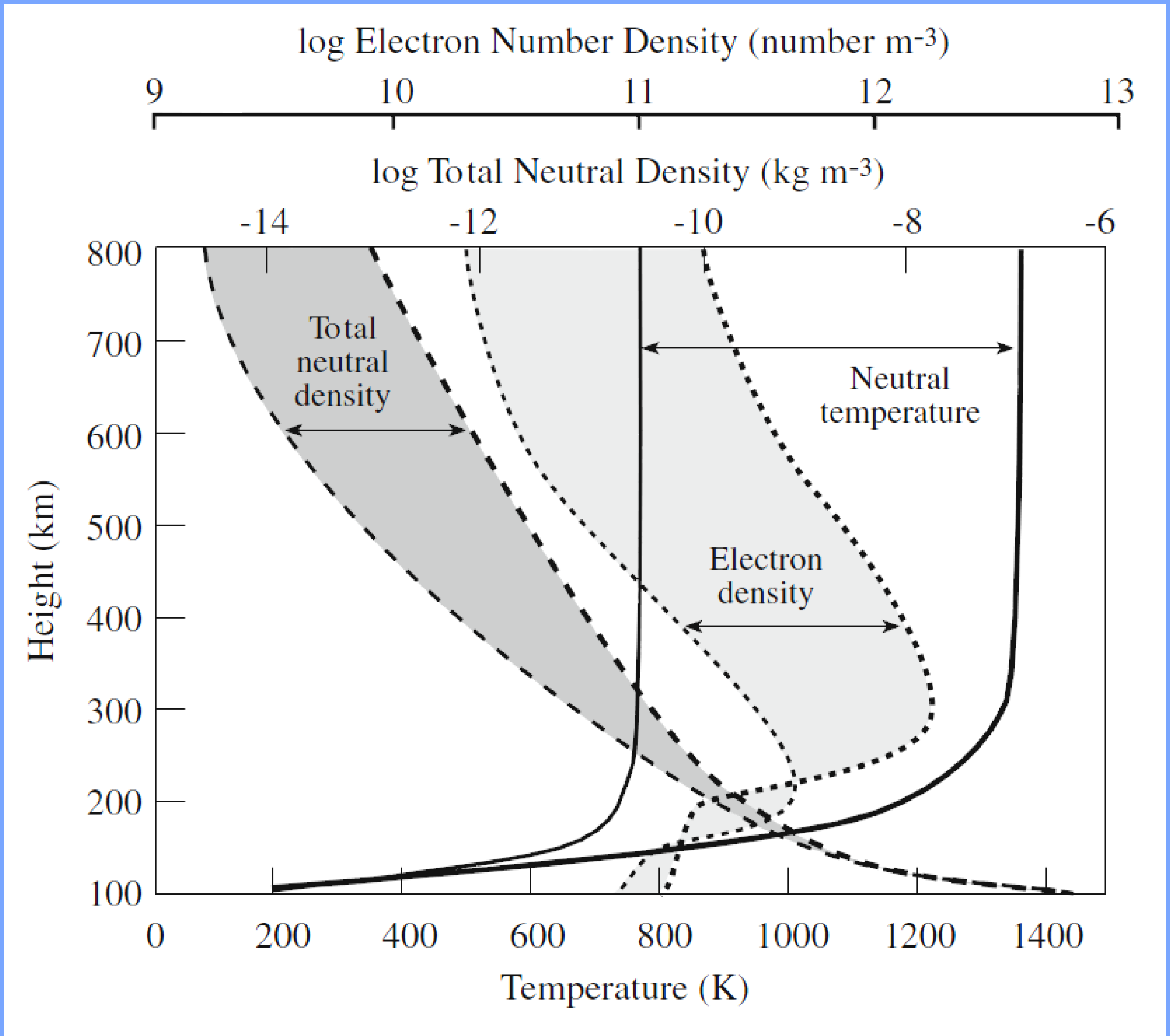

Lang, „The Sun from space"

Skutki rozbłysków słonecznych oraz ich wpływ na Ziemię i jej otoczenie

Struktura pola magnetycznego w przestrzeni międzyplanetarnej

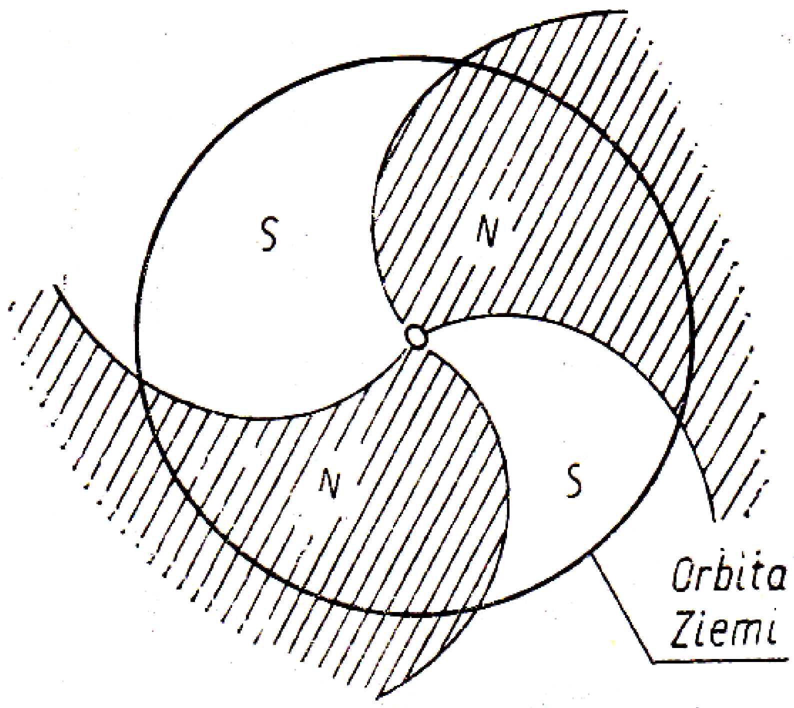

33. Sektorowa struktura pól magnetycznych w przestrzeni międzyplanetarnej (w polu oznaczonym *N* biegun północny jest skierowany ku Słońcu)

Mergentaler, „Słońce-Ziemia”

Skutki rozbłysków słonecznych oraz ich wpływ na Ziemię i jej otoczenie

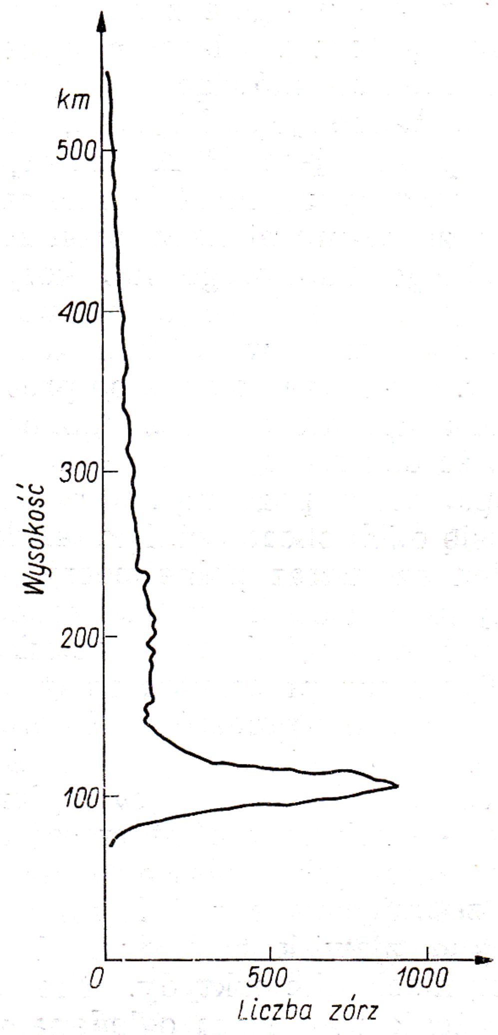

50. Częstość występowania zórz polarnych na różnych wysokościach w latach 1911—1944 (wg F. C. M. Störmera)

Występowanie zórz polarnych na różnych wysokościach (nad powierzchnią Ziemi).

Mergentaler, „Słońce-Ziemia”

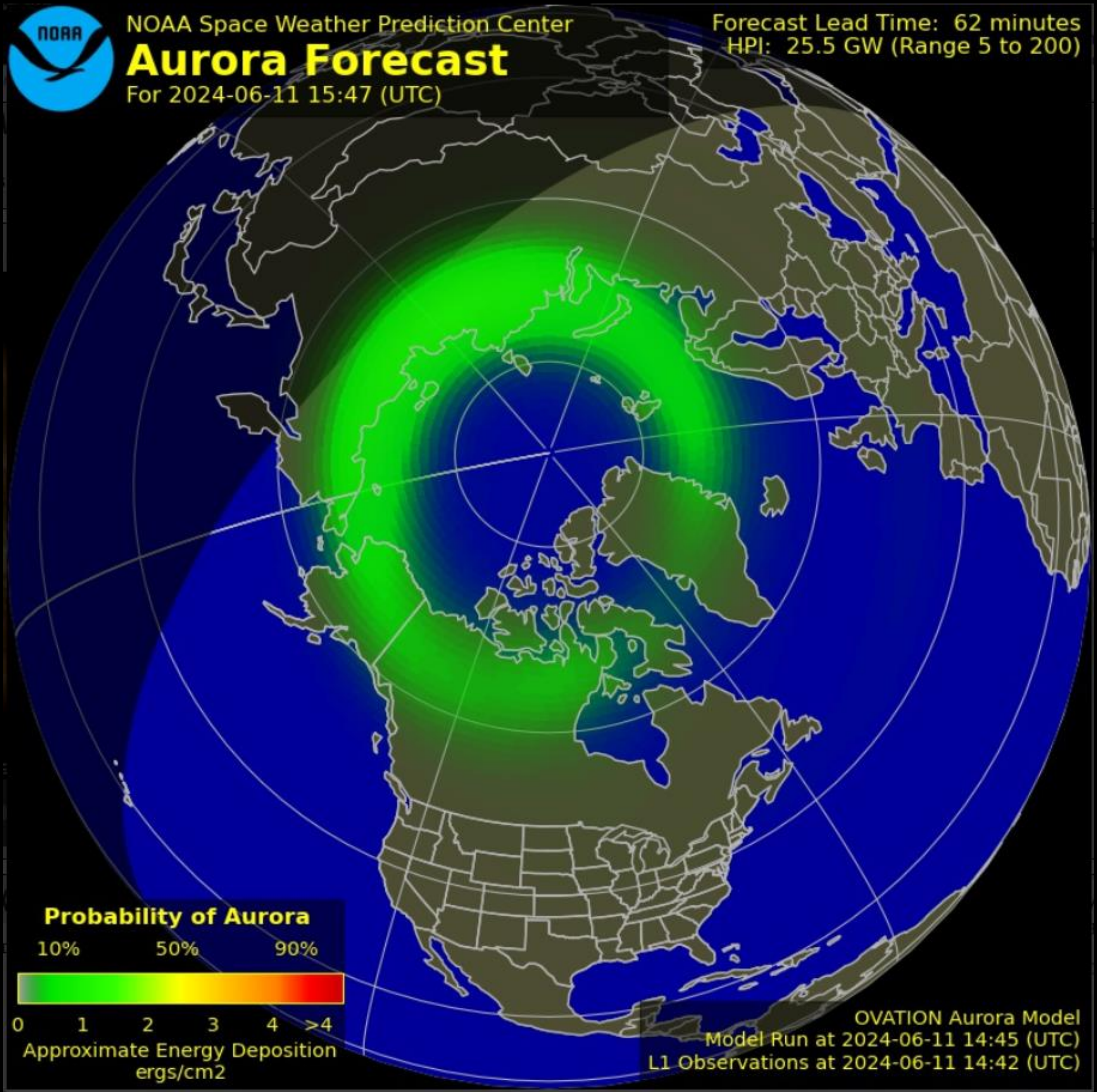
NOAA
NOAA Space Weather Prediction Center
Aurora Forecast
For 2024-06-11 15:47 (UTC)
Forecast Lead Time: 62 minutes
HPI: 25.5 GW (Range 5 to 200)
Probability of Aurora
10%
50%
90%
0
1
2
3
4
>4
Approximate Energy Deposition
ergs/cm2
OVATION Aurora Model
Model Run at 2024-06-11 14:45 (UTC)
L1 Observations at 2024-06-11 14:42 (UTC)

Rozbłyski gwiazdowe

Rozbłyski gwiazdowe

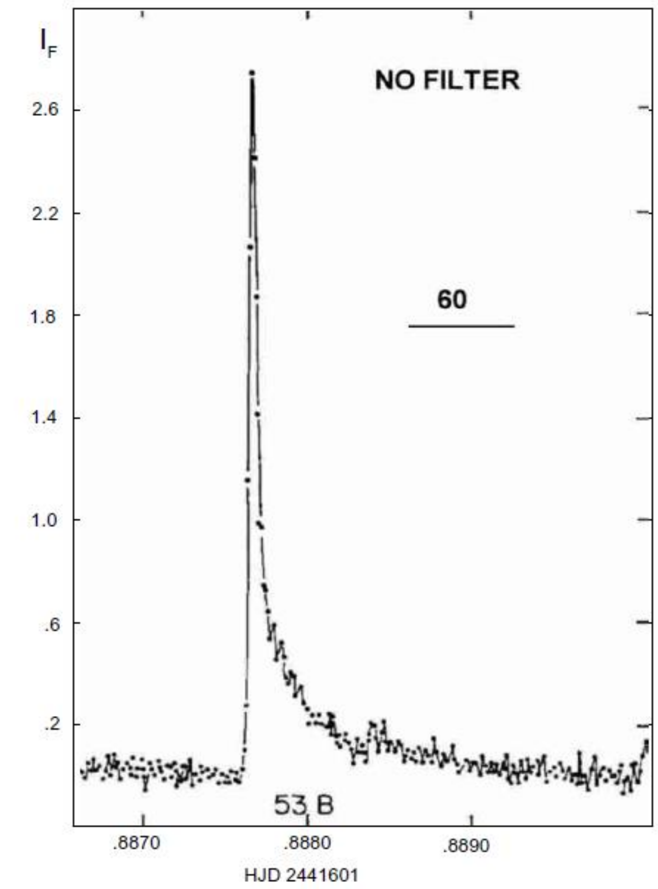

Fig. 1. The flare observed on UV Ceti (Moffett 1974b).

Rozbłyski gwiazdowe

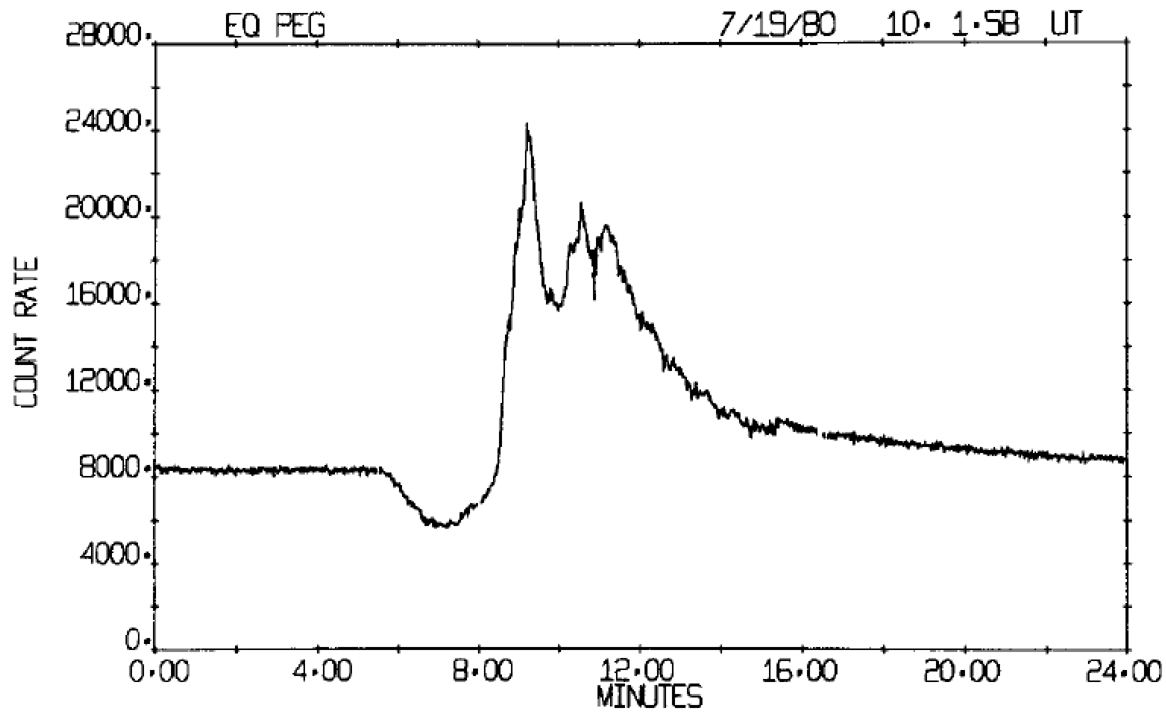

Figure 3. Flare event on a red dwarf flare star. A particularly striking example of the variety of phenomena that can be seen in stellar flares is encapsulated here in a single, extraordinary event observed on the binary flare star EQ Pegasi (dM3.5e + dM4.5e). This event was observed at the Cloudcroft Observatory 1.2 m utilizing high-speed photometry in the Johnson U band filter. The flare is preceded by a 'pre-flare dip', i.e. a decrease in the U band brightness of the star, in this case, of roughly 0.1 mag min^{-1} for 2.7 min. The signal then leveled off at 75% of the quiescent brightness for 1 min before the flare begins. The peak of the flare is 3 times the quiescent level brightness, and is followed by two more smaller peaks separated by 60 and 30 s. The flare event then decays exponentially in brightness, finally returning to the pre-flare level 19 min after the onset of the event. (From Giampapa M S, Africano J L, Klimke A, Parks J, Quigley R J, Robinson R D and Worden S P 1982 *Astrophys. J. Lett.* **252** L39.)

Rozbłyski gwiazdowe

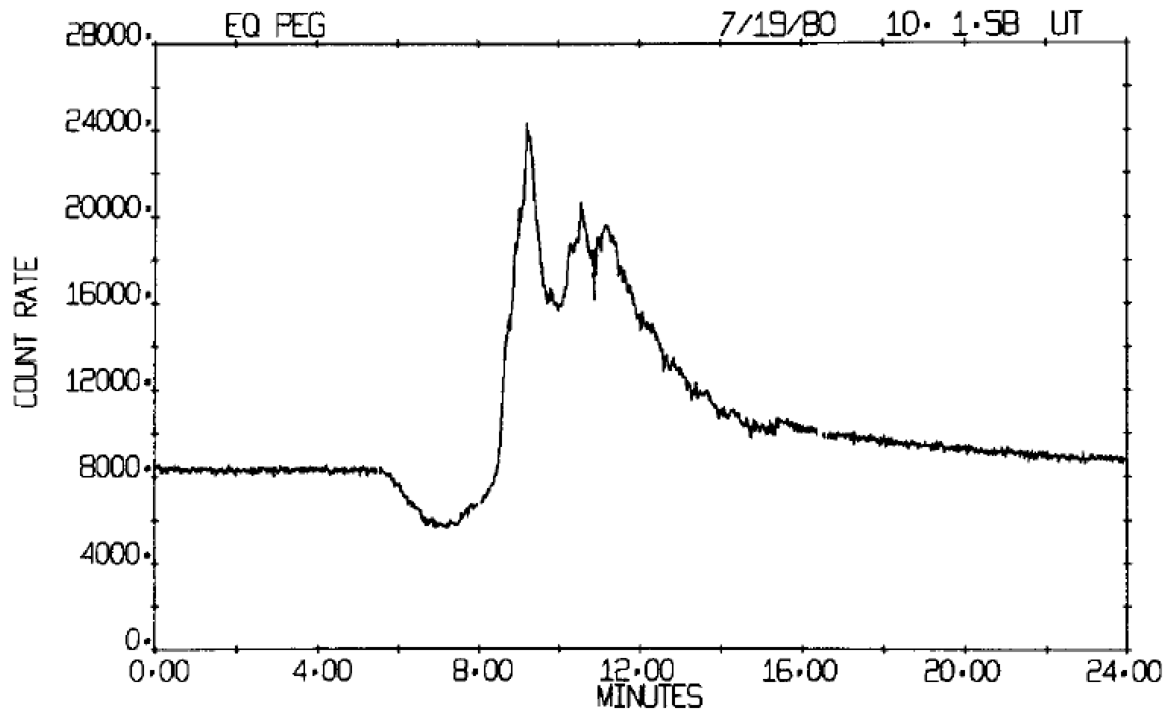

Figure 3. Flare event on a red dwarf flare star. A particularly striking example of the variety of phenomena that can be seen in stellar flares is encapsulated here in a single, extraordinary event observed on the binary flare star EQ Pegasi (dM3.5e + dM4.5e). This event was observed at the Cloudcroft Observatory 1.2 m utilizing high-speed photometry in the Johnson *U* band filter. The flare is preceded by a 'pre-flare dip', i.e. a decrease in the *U* band brightness of the star, in this case, of roughly 0.1 mag min^{-1} for 2.7 min. The signal then leveled off at 75% of the quiescent brightness for 1 min before the flare begins. The peak of the flare is 3 times the quiescent level brightness, and is followed by two more smaller peaks separated by 60 and 30 s. The flare event then decays exponentially in brightness, finally returning to the pre-flare level 19 min after the onset of the event. (From Giampapa M S, Africano J L, Klimke A, Parks J, Quigley R J, Robinson R D and Worden S P 1982 *Astrophys. J. Lett.* **252** L39.)

Rozbłyski gwiazdowe

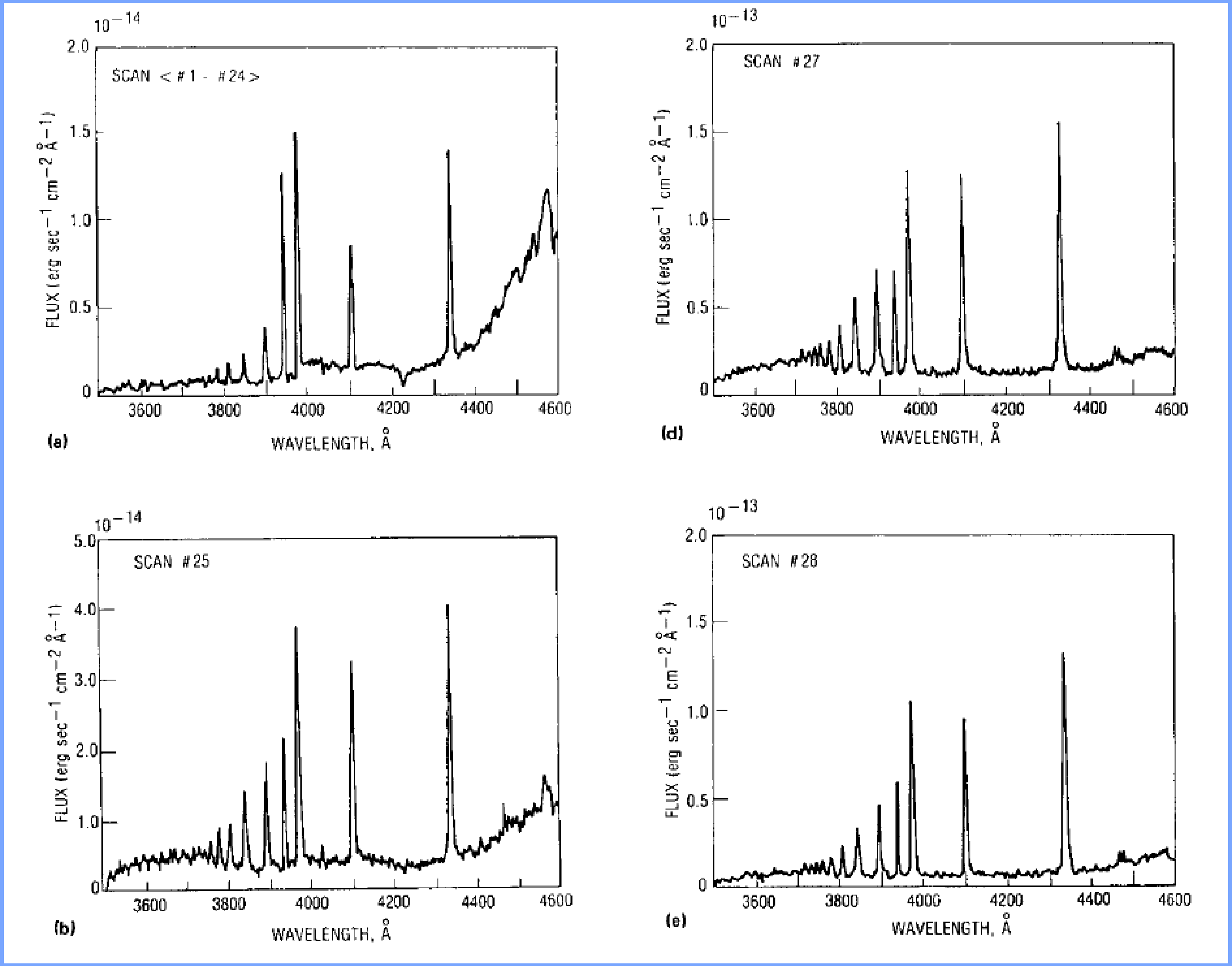

=>

gwiazdowe

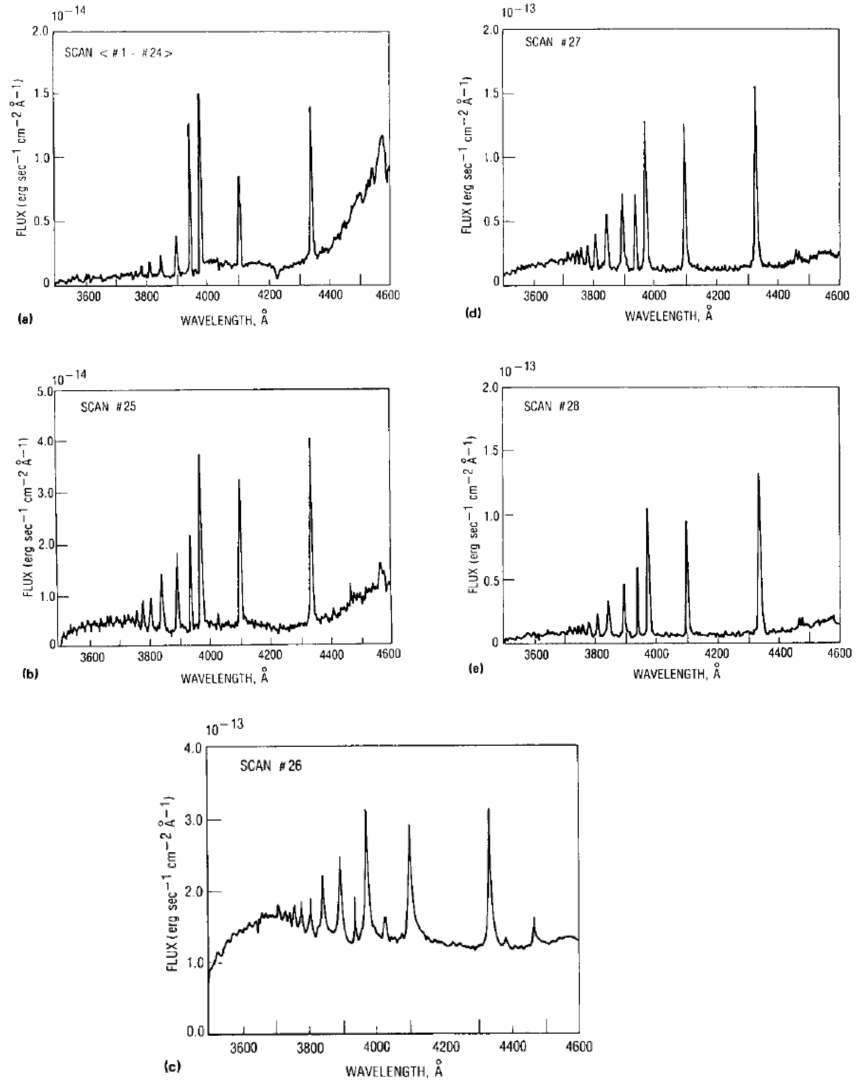

Figure 4. Spectrum of a large flare event. Time sequence of the blue spectrum of the flare star UV Ceti (dM5.6e) during the onset of a strong flare that exhibited a 5 mag increase in the photometric *U* band. The first scan is the average, quiescent spectrum of the star. The Ca II H and K lines are strong, and the Balmer series is evident out to H14, even during quiescence. The following scans document the onset of the flare event. Note the varying vertical axis scales. Emission lines from hydrogen are the most numerous and prominent emission features during the flare itself. Strong continuum emission is seen at the peak of the event in scan 26. Note the red asymmetry that appears in the emission lines at flare maximum, indicating the possible presence of mass motions. These spectra were originally obtained with the 2.3 m telescope and Reticon detector of the Steward Observatory of the University of Arizona. (From Eason E L E, Giampapa M S, Radick R R, Worden S P and Hege E K 1992 *Astron. J.* **104** 1161.)

Rozbłyski gwiazdowe

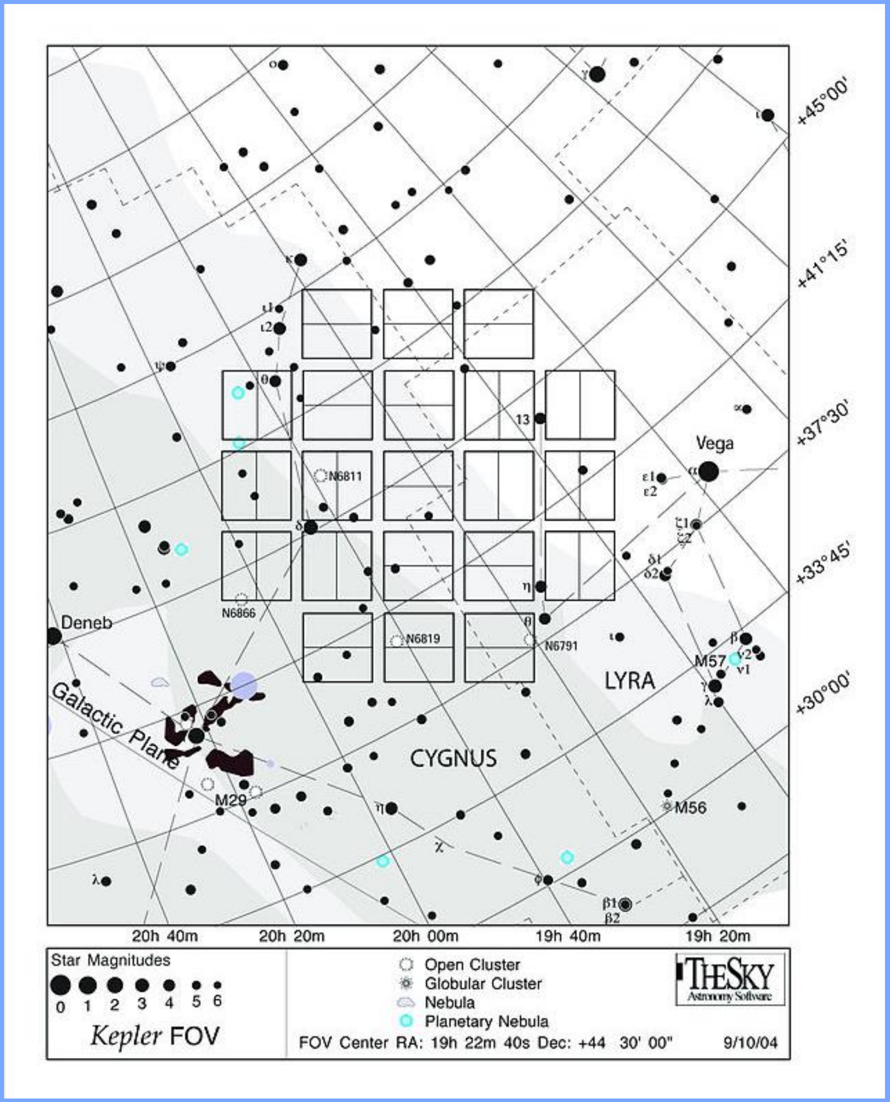

- Następnie (na skutek problemu z żyroskopami) obserwacje w pobliżu dysku Galaktyki

Lang, „The Sun from space”

Rozbłyski gwiazdowe

Astronomy & Astrophysics manuscript no. tinc
June 4, 2014

Kepler super-flare stars: what are they?

R. Wichmann[1], B. Fuhrmeister[1], U. Wolter[1], and E. Nagel[1]

Hamburger Sternwarte, Gojenbergsweg 112, 21029 Hamburg
e-mail: rwichmann@hs.uni-hamburg.de

Received date; Accepted date

ABSTRACT

The *Kepler* mission has led to the serendipitous discovery of a significant number of ‘super flares’ - white light flares with energies between 10^{33} erg and 10^{36} erg - on solar-type stars. It has been speculated that these could be ‘freak’ events that might happen on the Sun, too. We have started a programme to study the nature of the stars on which these super flares have been observed. Here we present high-resolution spectroscopy of 11 of these stars and discuss our results. We find that several of these stars are very young, fast-rotating stars where high levels of stellar activity can be expected, but for some other stars we do not find a straightforward explanation for the occurrence of super flares.

Key words. Stars: activity – Stars: chromospheres – Stars: flare – Stars: solar-type – Stars: rotation – Stars: atmospheres

Rozbłyski gwiazdowe

Astronomy & Astrophysics manuscript no. tinc
June 4, 2014

Kepler super-flare stars: what are they?

R. Wichmann[1], B. Fuhrmeister[1], U. Wolter[1], and E. Nagel[1]

Hamburger Sternwarte, Gojenbergsweg 112, 21029 Hamburg
e-mail: rwichmann@hs.uni-hamburg.de

Received date; Accepted date

ABSTRACT

The *Kepler* mission has led to the serendipitous discovery of a significant number of 'super flares' - white light flares with energies between 10^{33} erg and 10^{36} erg - on solar-type stars. It has been speculated that these could be 'freak' events that might happen on the Sun, too. We have started a programme to study the nature of the stars on which these super flares have been observed. Here we present high-resolution spectroscopy of 11 of these stars and discuss our results. We find that several of these stars are very young, fast-rotating stars where high levels of stellar activity can be expected, but for some other stars we do not find a straightforward explanation for the occurrence of super flares.

Key words. Stars: activity – Stars: chromospheres – Stars: flare – Stars: solar-type – Stars: rotation – Stars: atmospheres

Rozbłyski gwiazdowe

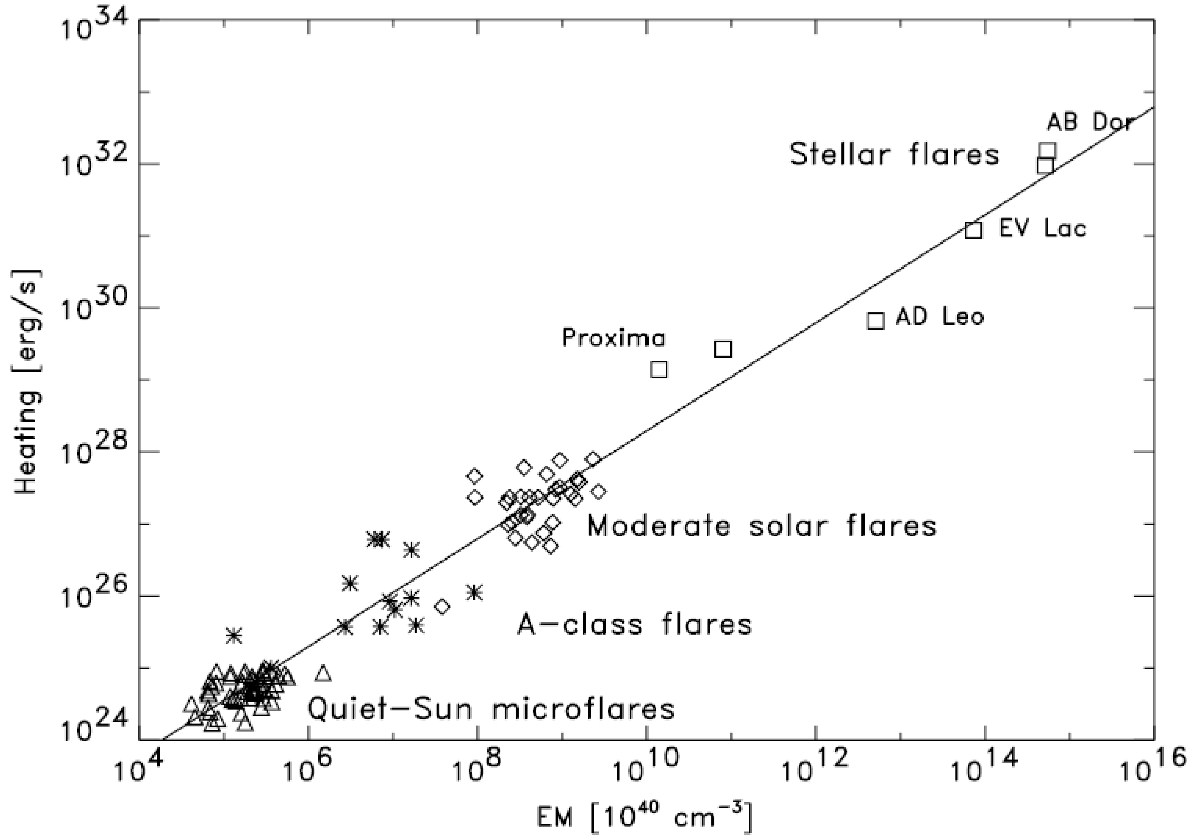

Fig. 1. Comparison of the heating rates observed in the flares of very different strengths. Triangles denote solar microflares, asterisks – A-class flares, diamonds – moderate and strong solar events and squares – the flares observed on active stars.

Preś i in., 2005

Rozbłyski gwiazdowe

Giant white-light flares on fully convective stars occur at high latitudes

Ekaterina Ilin[1,2], Katja Poppenhaeger[1,2], Sarah J. Schmidt[1], Silva P. Järvinen[1], Elisabeth R. Newton[3], Julián D. Alvarado-Gómez[1], J. Sebastian Pineda[4], James R. A. Davenport[5], Mahmoudreza Oshagh[6,7], Ilya Ilyin[1]
[1]Leibniz Institute for Astrophysics Potsdam (AIP), [2]University of Potsdam, [3]Dartmouth College, [4]University of Colorado Boulder, [5]University of Washington, [6]Instituto de Astrofísica de Canarias, [7]Universidad de La Laguna

submitted to MNRAS

In a **systematic analysis of fully convective stars observed with TESS**, we detected four stars that displayed giant **flares that were modulated in brightness by the stars' rapid rotation.** The morphology of the modulation allowed us to directly **localize these flares between 55° and 81° latitude on the stellar surface,** far higher than typical solar flare latitudes.

These findings are **a.** evidence that strong magnetic fields tend to emerge close to the stellar rotational poles for fully convective stars, and **b.** suggest that the impact of flares on the habitability of exoplanets around small stars could be weaker than previously thought.

data :: TESS light curves

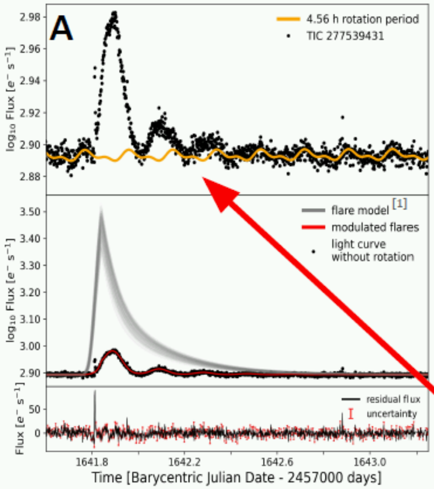

model :: rotational flare modulation

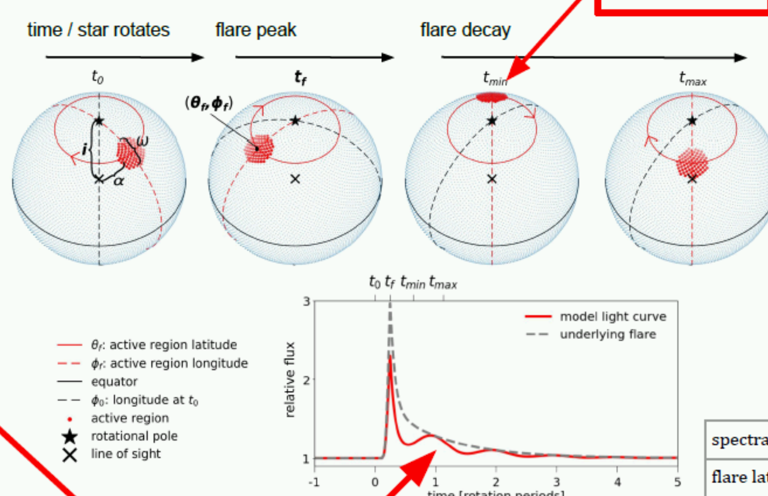

The flare flux is modulated while the active flaring region (partially) moves in and out of view on the stellar surface.

results :: high latitudes

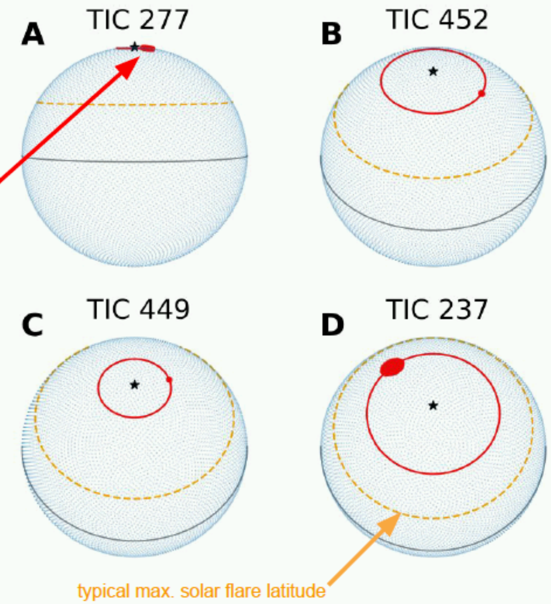

	A	B	C	D
spectral type	M7	M7	M6	M5
flare latitude [deg]	80.9 ± 0.5	63.1 ± 3.6	71.9 ± 1.1	55.2 ± 5.5
rotation period [h]	4.56	4.22	2.71	8.43
log(flare energy) [erg]	34.5	33.5	33.4	34.6

[1] Davenport et al. (2014), ApJ, 797, 122

AIP

Ekaterina Ilin
email: eilin@aip.de

Rozbłyski gwiazdowe

Monthly Notices of the ROYAL ASTRONOMICAL SOCIETY

MNRAS **504**, 3246–3264 (2021)
Advance Access publication 2021 April 14

doi:10.1093/mnras/stab979

Stellar flares detected with the Next Generation Transit Survey

James A. G. Jackman,[1,2,3★] Peter J. Wheatley,[1,2] Jack S. Acton,[4] David R. Anderson,[1,2] Daniel Bayliss,[1,2] Joshua T. Briegal,[5] Matthew R. Burleigh,[4] Sarah L. Casewell,[4] Boris T. Gänsicke,[1,2] Samuel Gill,[1] Edward Gillen,[5,6†] Michael R. Goad,[4] Maximilian N. Günther,[7‡] Beth A. Henderson,[4] Simon T. Hodgkin,[8] James S. Jenkins,[9,10] Chloe Pugh,[1] Didier Queloz,[5] Liam Raynard,[4] Rosanna H. Tilbrook,[4] Christopher A. Watson[11] and Richard G. West[1]

[1]*Department of Physics, University of Warwick, Gibbet Hill Road, Coventry CV4 7AL, UK*
[2]*Centre for Exoplanets and Habitability, University of Warwick, Gibbet Hill Road, Coventry CV4 7AL, UK*
[3]*School of Earth and Space Exploration, Arizona State University, Tempe, AZ 85287, USA*
[4]*School of Physics and Astronomy, University of Leicester, Leicester LE1 7RH, UK*
[5]*Astrophysics Group, Cavendish Laboratory, J.J. Thomson Avenue, Cambridge CB3 0HE, UK*
[6]*Astronomy Unit, Queen Mary University of London, Mile End Road, London E1 4NS, UK*
[7]*Department of Physics, and Kavli Institute for Astrophysics and Space Research, Massachusetts Institute of Technology, Cambridge, MA 02139, USA*
[8]*Institute of Astronomy, Madingley Road, Cambridge CB3 0HA, UK*
[9]*Departamento de Astronomia, Universidad de Chile, Camino El Observatorio 1515, Las Condes, Casilla 36-D, Santiago, Chile*
[10]*Centro de Astrofísica y Tecnologías Afines (CATA), Casilla 36-D, Santiago, Chile*
[11]*Astrophysics Research Centre, Queen's University of Belfast, 1 University Road, Belfast BT7 1NN, UK*

Accepted 2021 April 5. Received 2021 February 24; in original form 2020 December 23

ABSTRACT

We present the results of a search for stellar flares in the first data release from the Next Generation Transit Survey (NGTS). We have found 610 flares from 339 stars, with spectral types between F8 and M6, the majority of which belong to the Galactic thin disc. We have used the 13 s cadence NGTS light curves to measure flare properties such as the flare amplitude, duration, and bolometric energy. We have measured the average flare occurrence rates of K and early to mid-M stars and present a generalized method to measure these rates while accounting for changing detection sensitivities. We find that field age K and early M stars show similar flare behaviour, while fully convective M stars exhibit increased white-light flaring activity, which we attribute to their increased spin-down time. We have also studied the average flare rates of pre-main-sequence K and M stars, showing they exhibit increased flare activity relative to their main-sequence counterparts.

Rozbłyski gwiazdowe

Cool Stars 20.5

Statstical Properties of Superflares on Solar-type Stars: Results Using All of the Kepler Primary Mission Data

Soshi Okamoto[1]; Yuta Notsu[2]; Hiroyuki Maehara[3]; Kosuke Namekata[1]; Kai Ikuta[1]; Daisaku Nogami[1]; Kazunari Shibata[1]; Satoshi Honda[4]
[1]Kyoto University; [2]University of Colorado Boulder; [3]NAOJ; [4]University of Hyogo

Solar flares are energetic explosions in the solar atmosphere, and superflares are the flares having the energy 10 - 10^6 times larger than that of the largest solar flare. Recently, many superflares on solar-type (G-type main-sequence; effective temperature is 5100 – 6000 K) stars were found in the initial 500 days data obtained by the Kepler spacecraft (Maehara et al. 2012; Shibayama et al. 2013). Notsu et al. (2019) conducted precise measurements and binarity check on the basis of spectroscopic observations and the Gaia-DR2 data. As a result, the number of Sun-like (effective temperature is 5600 – 6000 K and rotation period is over 20 days) superflare stars significantly decreased.
We report the latest statistical analyses of superflares on solar-type stars using all of the Kepler primary mission data and Gaia-DR2 catalog. We updated the flare detection method by using highpass filter to remove rotational variations caused by starspots. We also examined the sample biases on the frequency of superflares, taking into account gyrochronology and flare detection completeness. The sample size of solar-type stars and Sun-like stars are ~4 and ~12 times, respectively, compared with Notsu et al. (2019). As a result, we found 2341 superflares on 265 solar-type stars, and 26 superflares on 15 Sun-like stars. This enabled us to have a more well-established view on the statistical properties of superflares. The observed upper limit of the flare energy decreases as the rotation period increases in solar-type stars. The frequency of superflares decreases as the stellar rotation period increases. The maximum energy we found on Sun-like stars is 4×10^{34} erg. Our analysis of Sun-like stars suggest that the Sun can cause superflares with energies of 7×10^{33} erg (~X700-class flares) and $\sim 1 \times 10^{34}$ erg (~X1000-class flares) once every ~3,000 years and ~6,000 years, respectively (Okamoto et al. 2021).

1. Can our Sun produce superflares?

Superflares are the flares having energy 10 – 10^6 times larger than that of the largest solar flares (~ 10^{32} erg)

Large solar flares can have severe impacts on our Earth.
We do not know the superflares occur on our Sun with only modern solar observations (since 1859).
→Using the data of solar-type (G-main sequence) stars!

2. Discoveries of superflares with initial Kepler data

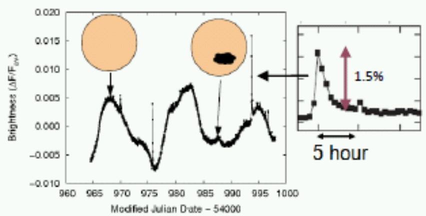

[Maehara+2012, Shibayama+2013]
We discovered more than 1,000 superflares on ~300 solar-type (G-type main sequence) stars from initial Kepler ~500 days data.

[Notsu+2019]
Removing contamination of subgiants, using stellar radius updates from Gaia-DR2
→ The number of superflares are much smaller than Shibayama+2013.

3. Superflare analysis using all of the Kepler data

[Okamoto+2021]
- Including stars previously identified as subgiants but newly as main-sequence thanks to Gaia-DR2 data.
- Using all the Kepler data of 4-years and Gaia-DR2 data

→The total size of analyzed data of Sun-like stars (P_{rot} > 20 day, 5600-6000K) is ~12 times compare to Notsu+2019.

	Number of all stars	Number of superflare stars	Number of superflares
Solar-type stars (5100-6000K)	11601	265(113)	2341(527)
Solar-type stars with 5600-6000K	5074	117(45)	929(154)
Sun-like stas (20 day<P_{rot}, 5600-6000K)	1641	15(3)	26(3)

*Sun:T~5780,P_{rot}~25days **Number in "()" are those in Notsu+2019

4. Dependence on rotational period of solar-type stars

Rotation Period vs Flare energy

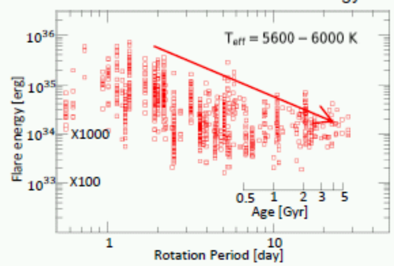

Rotation Period vs Flare Frequency

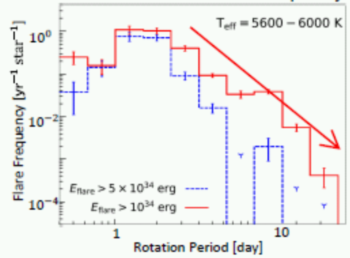

Upper limit of flare energy slightly depends on the rotation period.

Flare frequency also decreases as rotation period increases (Prot > 2-3 days).

Superflare analysis solar-type stars (G-type main sequence, 5100-6000K)

- Even Sun-like stars (5600-6000K, Prot > 20 days, Age~4.6Gyr) can have superflares up to 5 × 10^{34} erg.
- Young rapidly-rotating stars (Prot ~ 2-3 days, Age~a few hundreds Myr) can have superflares up to 10^{36} erg and flare frequency is ~100 times larger than slowly-rotating Sun-like stars.

5. The large starspots are needed to occur superflares

Rotation period vs star spot area

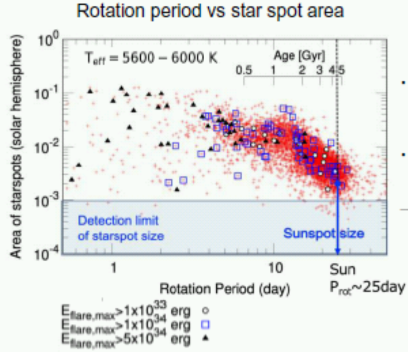

- Large starsopts (~1% of solar hemisphere) still can exist on slowly-rotating Sun-like stars(5600-6000K, Prot > 20 days, Age~4.6 Gyr).
- Superflares are occur on the stars with large starspots.

→Magnetic energy is necessary for superflares.

6. Freqency distribution of superflares on Sun-like stars and solar flares

Flare energy vs Flare Frequency

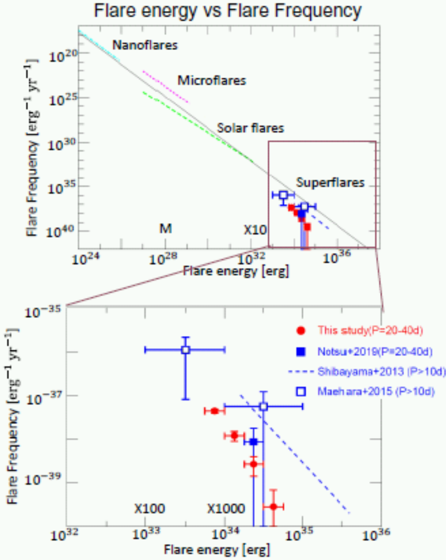

From Sun-like stars (5600-6000K, Prot > 20 days), the Sun can produce superflares:
~ 7×10^{33} erg, X700 class : once in 3000 years
~ 1×10^{34} erg, X1000 class : once in 6000 years

- Many superflares (>2000) on many solar-type (G-type main sequence) stars (>265) were discovered from all the Kepler 4-year data and Gaia-DR2 data.
- Flare activities depends on stellar age (rotation period). Young rapidly-rotating stars have more frequent and energetic flares than Sun-like stars (Prot > 20 days).
- From Sun-like stars analysis, (5600-6000K, Prot > 20 days) our Sun can occur superflares
  ~ 7×10^{33} erg X700 class : once in 3000 years
  ~ 1×10^{34} erg, X1000 class : once in 6000 years

Okamoto et al. 2021, ApJ, 906, 72: https://ui.adsabs.harvard.edu/abs/2021ApJ...906...72O/abstract

Rozbłyski gwiazdowe

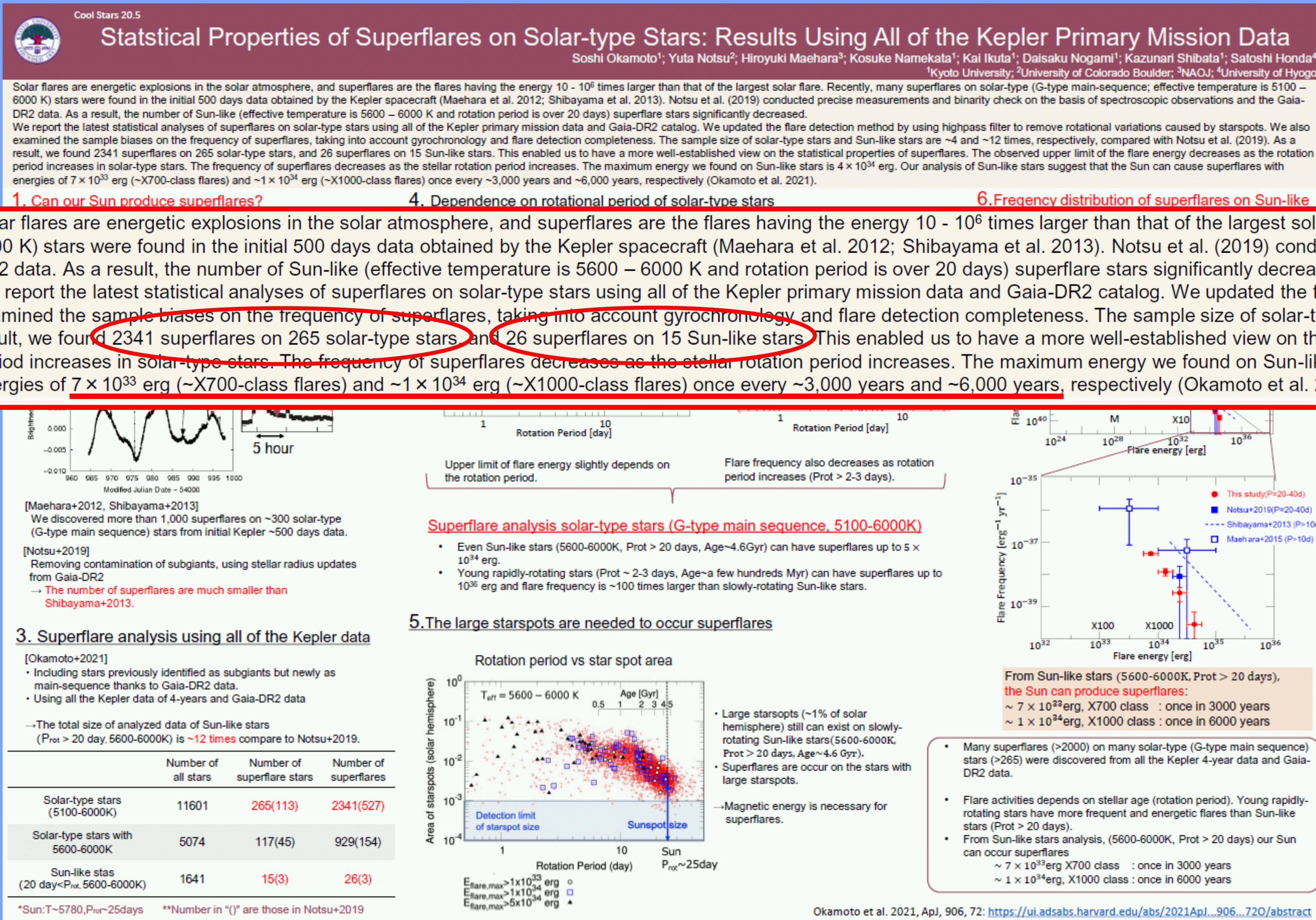

Cool Stars 20.5

Statstical Properties of Superflares on Solar-type Stars: Results Using All of the Kepler Primary Mission Data

Soshi Okamoto[1]; Yuta Notsu[2]; Hiroyuki Maehara[3]; Kosuke Namekata[1]; Kai Ikuta[1]; Daisaku Nogami[1]; Kazunari Shibata[1]; Satoshi Honda[4]
[1]Kyoto University; [2]University of Colorado Boulder; [3]NAOJ; [4]University of Hyogo

Solar flares are energetic explosions in the solar atmosphere, and superflares are the flares having the energy 10 - 10^6 times larger than that of the largest solar flare. Recently, many superflares on solar-type (G-type main-sequence; effective temperature is 5100 – 6000 K) stars were found in the initial 500 days data obtained by the Kepler spacecraft (Maehara et al. 2012; Shibayama et al. 2013). Notsu et al. (2019) conducted precise measurements and binarity check on the basis of spectroscopic observations and the Gaia-DR2 data. As a result, the number of Sun-like (effective temperature is 5600 – 6000 K and rotation period is over 20 days) superflare stars significantly decreased.
We report the latest statistical analyses of superflares on solar-type stars using all of the Kepler primary mission data and Gaia-DR2 catalog. We updated the flare detection method by using highpass filter to remove rotational variations caused by starspots. We also examined the sample biases on the frequency of superflares, taking into account gyrochronology and flare detection completeness. The sample size of solar-type stars and Sun-like stars are ~4 and ~12 times, respectively, compared with Notsu et al. (2019). As a result, we found 2341 superflares on 265 solar-type stars, and 26 superflares on 15 Sun-like stars. This enabled us to have a more well-established view on the statistical properties of superflares. The observed upper limit of the flare energy decreases as the rotation period increases in solar-type stars. The frequency of superflares decreases as the stellar rotation period increases. The maximum energy we found on Sun-like stars is 4×10^{34} erg. Our analysis of Sun-like stars suggest that the Sun can cause superflares with energies of 7×10^{33} erg (~X700-class flares) and ~1×10^{34} erg (~X1000-class flares) once every ~3,000 years and ~6,000 years, respectively (Okamoto et al. 2021).

Solar flares are energetic explosions in the solar atmosphere, and superflares are the flares having the energy 10 - 10^6 times larger than that of the largest solar flare
6000 K) stars were found in the initial 500 days data obtained by the Kepler spacecraft (Maehara et al. 2012; Shibayama et al. 2013). Notsu et al. (2019) conducted
DR2 data. As a result, the number of Sun-like (effective temperature is 5600 – 6000 K and rotation period is over 20 days) superflare stars significantly decreased.
We report the latest statistical analyses of superflares on solar-type stars using all of the Kepler primary mission data and Gaia-DR2 catalog. We updated the flare de
examined the sample biases on the frequency of superflares, taking into account gyrochronology and flare detection completeness. The sample size of solar-type sta
result, we found 2341 superflares on 265 solar-type stars, and 26 superflares on 15 Sun-like stars. This enabled us to have a more well-established view on the stati
period increases in solar-type stars. The frequency of superflares decreases as the stellar rotation period increases. The maximum energy we found on Sun-like star
energies of 7×10^{33} erg (~X700-class flares) and ~1×10^{34} erg (~X1000-class flares) once every ~3,000 years and ~6,000 years, respectively (Okamoto et al. 2021).

1. Can our Sun produce superflares?

[Maehara+2012, Shibayama+2013]
We discovered more than 1,000 superflares on ~300 solar-type (G-type main sequence) stars from initial Kepler ~500 days data.

[Notsu+2019]
Removing contamination of subgiants, using stellar radius updates from Gaia-DR2
→ The number of superflares are much smaller than Shibayama+2013.

3. Superflare analysis using all of the Kepler data

[Okamoto+2021]
- Including stars previously identified as subgiants but newly as main-sequence thanks to Gaia-DR2 data.
- Using all the Kepler data of 4-years and Gaia-DR2 data

→The total size of analyzed data of Sun-like stars (P_{rot} > 20 day, 5600-6000K) is ~12 times compare to Notsu+2019.

	Number of all stars	Number of superflare stars	Number of superflares
Solar-type stars (5100-6000K)	11601	265(113)	2341(527)
Solar-type stars with 5600-6000K	5074	117(45)	929(154)
Sun-like stas (20 day<P_{rot}, 5600-6000K)	1641	15(3)	26(3)

*Sun:T~5780,P_{rot}~25days **Number in "()" are those in Notsu+2019

4. Dependence on rotational period of solar-type stars

Upper limit of flare energy slightly depends on the rotation period.

Flare frequency also decreases as rotation period increases (Prot > 2-3 days).

Superflare analysis solar-type stars (G-type main sequence, 5100-6000K)

- Even Sun-like stars (5600-6000K, Prot > 20 days, Age~4.6Gyr) can have superflares up to 5×10^{34} erg.
- Young rapidly-rotating stars (Prot ~ 2-3 days, Age~a few hundreds Myr) can have superflares up to 10^{36} erg and flare frequency is ~100 times larger than slowly-rotating Sun-like stars.

5. The large starspots are needed to occur superflares

Rotation period vs star spot area

- Large starsopts (~1% of solar hemisphere) still can exist on slowly-rotating Sun-like stars(5600-6000K, Prot > 20 days, Age~4.6 Gyr).
- Superflares are occur on the stars with large starspots.

→Magnetic energy is necessary for superflares.

6. Freqency distribution of superflares on Sun-like

From Sun-like stars (5600-6000K, Prot > 20 days), the Sun can produce superflares:
~ 7×10^{33} erg, X700 class : once in 3000 years
~ 1×10^{34} erg, X1000 class : once in 6000 years

- Many superflares (>2000) on many solar-type (G-type main sequence) stars (>265) were discovered from all the Kepler 4-year data and Gaia-DR2 data.
- Flare activities depends on stellar age (rotation period). Young rapidly-rotating stars have more frequent and energetic flares than Sun-like stars (Prot > 20 days).
- From Sun-like stars analysis, (5600-6000K, Prot > 20 days) our Sun can occur superflares
  ~ 7×10^{33} erg X700 class : once in 3000 years
  ~ 1×10^{34} erg, X1000 class : once in 6000 years

Okamoto et al. 2021, ApJ, 906, 72: https://ui.adsabs.harvard.edu/abs/2021ApJ...906...72O/abstract

Rozbłyski gwiazdowe

MNRAS 000, 1–5 () Preprint 1 June 2021 Compiled using MNRAS LaTeX style file v3.0

Characteristic time of stellar flares on Sun-like stars

Y. Yan,[1,2,6,7]★ H. He,[1,2,8]★ C. Li,[3,7] A. Esamdin,[4,8]
B. L. Tan,[1,2,8] L. Y. Zhang[5] and H. Wang[6]
[1] *National Astronomical Observatories, Chinese Academy of Sciences, Beijing 100101, China*
[2] *CAS Key Laboratory of Solar Activity, Chinese Academy of Sciences, Beijing 100101, China*
[3] *School of Astronomy and Space Science, Nanjing University, Nanjing 210023, China*
[4] *Xinjiang Astronomical Observatory, Chinese Academy of Sciences, Urumqi 830011, China*
[5] *College of Physics, and College of Big Data and Information Engineering, Guizhou University, Guiyang 550025, China*
[6] *Center for Solar-Terrestrial Research, New Jersey Institute of Technology, University Heights, Newark, NJ 07102-1982, USA*
[7] *Key Laboratory for Modern Astronomy and Astrophysics, Ministry of Education, Nanjing 210023, China*
[8] *University of Chinese Academy of Sciences, Beijing 100049, China*

Accepted XXX. Received YYY; in original form ZZZ

ABSTRACT

Using the short cadence data (1-minute interval) of the *Kepler* space telescope, we conducted a statistical analysis for the characteristic time of stellar flares on Sun-like stars (SLS). Akin to solar flares, stellar flares show rise and decay light curve profile, which reflects two distinct phases (rise phase and decay phase) of flare process. We derived the characteristic times of the two phases for the stellar flares of SLS, resulting the median rise time of about 5.9 minutes and the median decay time of 22.6 minutes. It is found that both the rise time and the decay time of the stellar flares follow the log-normal distribution. The peak positions of the log-normal distributions for flare rise time and decay time are 3.5 minutes and 14.8 minutes, respectively. These time values of stellar flares are similar to the timescale of solar flares, which supports that stellar flares and solar flares have the same physical mechanism. The statistical results obtained in this work for SLS can be a benchmark of flare characteristic times when comparing with other types of stars.

Key words: Stars: activity – Stars: flare – Stars: solar-type

wykres =>

Rozbłyski gwiazdowe

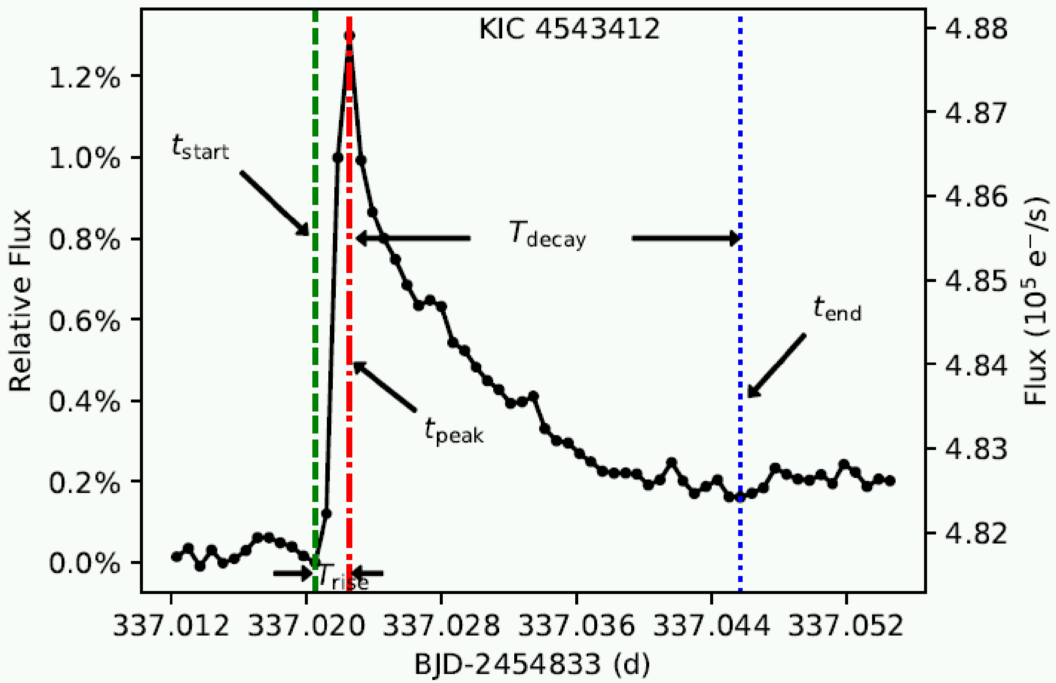

Figure 1. An example flare light curve of SLS (KIC4543412) observed in *Kepler* SC mode. The dots in the curve represent the SC data points with 1-minute interval. The time parameters (t_{start}, t_{peak}, t_{end}, T_{rise}, and T_{decay}) of the flare are marked in the plot. The percentage value of the flare intensity enhancement (relative flux) shown in the left Y-axis is relative to the absolute flux value (shown in the right Y-axis) at the time of t_{start}. BJD in the X-axis means Barycentric Julian Date. The offset 2,454,833 is the Julian Date on 2009 January 1.

Do powyższych (jednych z pierwszych, ciekawych) opracowań dotyczących obserwacji rozbłysków gwiazdowych należy dodać osiągnięcia w badaniach tego typu zjawisk z ostatnich lat - w tym prace wykonane w naszym instytucie (ostatnie dwa lata). W ostatnich latach liczba prac dotycząca rozbłysków gwiazdowych wzrasta „lawinowo” =>

https://ui.adsabs.harvard.edu/classic-form

https://ui.adsabs.harvard.edu/search/fq=%7B!type%3Daqp%20v%3D%24fq_database%7D&fq_database=database%3A%20astronomy&q=title%3A(stellar%20flare)&sort=date%20desc%2C%20bibcode%20desc&p_=0

Fizyka rozbłysków słonecznych

KONIEC

Krzysztof Radziszewski

Instytut Astronomiczny, Uniwersytet Wrocławski